25. Strelow A, Bernardo K, Adam-Klages S, Linke T, Sandhoff K, Kronke M and Adam D (2000) Overexpression of acid ceramidase protects from tumor necrosis factor-induced cell death. J. Exp. Med. 192: 601–612
26. Harel R and Futerman AH (1993) Inhibition of sphingolipid synthesis affects axonal outgrowth in cultured hippocampal neurons. J. Biol. Chem. 268: 14476–14481
27. Chen JJ, Reid CE, Band V and Androphy EJ (1995) Interaction of papillomavirus E6 oncoproteins with a putative calcium-binding protein. Science 269: 529–531
28. Tong X and Howley PM (1997) The bovine papillomavirus E6 oncoprotein interacts with paxillin and disrupts the actin cytoskeleton. Proc. Natl. Acad. Sci. USA 94: 4412–4417
29. Gao Q, Srinivasan S, Boyer S, Wazer D and Band V (1999) The E6 oncoproteins of high-risk papillomaviruses bind to a novel putative GAP protein, E6TP1, and target it for degradation. Mol. Cell. Biol. 19: 733–744
30. Zimmermann H, Degenkolbe R, Bernard HU and O'Connor MJ (1999) The human papillomavirus type 16 E6 oncoprotein can down-regulate p53 activity by targeting the transcriptional coactivator CBP/p300. J. Viol. 73: 6209–6219
31. Gao Q, Kumar A, Srinivasan S, Singh L, Mukai H, Ono Y, Wazer DE and Band V (2000) PKN binds and phosphorylates human papillomavirus E6 oncoprotein. J. Biol. Chem. 275: 14824–14830
32. Jayadev S, Liu B, Bielawska A, Lee J, Nazaire F, Pushkareva MY, Obeid L and Hannun YA (1995) Role for ceramide in cell cycle arrest. J. Biol. Chem. 270: 2047–2052
33. Yoshimura S, Banno Y, Nakashima S, Takenaka K, Sakai H, Nishimura Y, Sakai N, Shimizu S, Eguchi Y, Tsujimoto Y and Nozawa Y (1998) Ceramide formation leads to caspase-3 activation during hypoxic PC12 cell death. J. Biol. Chem. 273: 6921–6927
34. Takeda Y, Tashima M, Takahashi A, Uchiyama T and Okazaki T (1999) Ceramide generation in nitric oxide-induced apoptosis. Activation of magnesium-dependent neutral sphingomyelinase via caspase-3. J. Biol. Chem. 274: 10654–10660
35. Jaffrezou JP, Levade T, Bettaieb A, Andrieu N, Bezombes C, Maestre N, Vermeersch S, Rousse A and Laurent G (1996) Daunorubicin-induced apoptosis: triggering of ceramide generation through sphingomyelin hydrolysis. EMBO J. 15: 2417–2424
36. Santana P, Pena LA, Haimovitz-Friedman A, Martin S, Green D, McLoughlin M, Cordon-Cardo C, Schuchman EH, Fuks Z and Kolesnick R (1996) Acid sphingomyelinase-deficient human lymphoblasts and mice are defective in radiation-induced apoptosis. Cell 86: 189–199
37. Cifone MG, De Maria R, Roncaioli P, Rippo MR, Azuma M, Lanier LL, Santoni A and Testi R (1994) Apoptotic signaling through CD95 (Fas/Apo-1) activates an acidic sphingomyelinase. J. Exp. Med. 180: 1547–1552
38. Schwandner R, Wiegmann K, Bernardo K, Kreder D and Kronke M (1998) TNF receptor death domain-associated proteins TRADD and FADD signal activation of acid sphingomyelinase. J. Biol. Chem. 273: 5916–5922
39. Chmura SJ, Nodzenski E, Beckett MA, Kufe DW, Quintans J and Weichselbaum RR (1997) Loss of ceramide production confers resistance to radiation-induced apoptosis. Cancer Res. 57: 1270–1275
40. Alphonse G, Aloy MT, Broquet P, Gerard JP, Louisot P, Rousson R and Rodriguez-Lafrasse C (2002) Ceramide induces activation of the mitochondrial/caspases pathway in Jurkat and SCC61 cells sensitive to γ-radiation but activation of this sequence is defective in radioresistant SQ20B cells. Int. J. Radiat. Biol. 78: 821–835
41. Kimura K, Markowski M, Edsall LC, Spiegel S and Gelmann EP (2003) Role of ceramide in mediating apoptosis of irradiated LNCaP prostate cancer cells. Cell Death Differ. 10: 240–248
42. Cuvillier O, Pirianov G, Kleuser B, Vanek PG, Coso OA, Gutkind S and Spiegel S (1996) Suppression of ceramide-mediated programmed cell death by sphingosine-1-phosphate. Nature 381: 800–803
43. An S, Zheng Y and Bleu T (2000) Sphingosine 1-phosphate-induced cell proliferation, survival, and related signaling events mediated by G protein-coupled receptors Edg3 and Edg5. J. Biol. Chem. 275: 288–296
44. Osawa Y, Banno Y, Nagaki M, Brenner DA, Naiki T, Nozawa Y, Nakashima S and Moriwaki H (2001) TNF-α-induced sphingosine 1-phosphate inhibits apoptosis through a phosphatidylinositol 3-kinase/Akt pathway in human hepatocytes. J. Immunol. 167: 173–180
45. Takeda Y, Mori T, Imabayashi H, Kiyono T, Gojo S, Miyoshi S, Ita M, Segawa K, Ogawa S, Sakamoto M, Nakamura S and Umezawa A (2004) Can the lifespan of human marrow stromal cells be prolonged by bim-1, E6, E7, and/or telomerase without affecting cardiomyogenic differentiation? J. Gene Med., (in press).

THE JOURNAL OF GENE MEDICINE
J Gene Med 2004; 6: 833–845.
Published online 30 March 2004 in Wiley InterScience (www.interscience.wiley.com). DOI: 10.1002/jgm.583

RESEARCH ARTICLE

Can the life span of human marrow stromal cells be prolonged by bmi-1, E6, E7, and/or telomerase without affecting cardiomyogenic differentiation?

Yukiji Takeda,[1,2,3] Taisuke Mori,[1,2] Hideaki Imabayashi,[1,4] Tohru Kiyono,[5] Satoshi Gojo,[6] Shunichirou Miyoshi,[7] Naoko Hida,[1,2] Makoto Ita,[8] Kaoru Segawa,[9] Satoshi Ogawa,[7] Michiie Sakamoto,[2] Shinobu Nakamura,[3] Akihiro Umezawa[1]*

[1]*Department of Reproductive Biology and Pathology, National Research Institute for Child Health and Development, Tokyo, Japan;* [2]*Department of Pathology, Keio University School of Medicine, Tokyo, Japan;* [3]*Department of General Medicine and Clinical Investigation, Nara Medical University, Nara, Japan;* [4]*Department of Orthopedics, Keio University School of Medicine, Tokyo, Japan;* [5]*Virology Division, National Cancer Center Research Institute, Tokyo, Japan;* [6]*Department of Cardiovascular Surgery, Saitama Medical Center, Kawagoe, Japan;* [7]*Cardiopulmonary Division, Department of Internal Medicine, Keio University School of Medicine, Tokyo, Japan;* [8]*Pharmacia-Keio Research Laboratories, Shinanomachi Research Park, Keio University School of Medicine, Tokyo, Japan;* [9]*Department of Virology, Keio University School of Medicine, Tokyo, Japan*

*Correspondence to: Akihiro Umezawa, Department of Reproductive Biology and Pathology, National Research Institute for Child Health and Development, Okura, Setagaya, Tokyo, 157-8535 Japan. E-mail: umezawa@1985.jukuin.keio.ac.jp

Received: 23 May 2003
Revised: 16 October 2003
Accepted: 27 January 2004

Abstract

Background Cell transplantation has recently been challenged to improve cardiac function of severe heart failure. Human mesenchymal stem cells (hMSCs) are multipotent cells that can be isolated from adult marrow stroma, but because of their limited life span, it is difficult to study them further. To overcome this problem, we attempted to prolong the life span of hMSCs and investigate whether the hMSCs modified with cell-cycle-associated genes can differentiate into cardiomyocytes *in vitro*.

Methods We attempted to prolong the life span of hMSCs by infecting retrovirus encoding bmi-1, human papillomavirus E6 and E7, and/or human telomerase reverse transcriptase genes. To determine whether the hMSCs with an extended life span could differentiate into cardiomyocytes, 5-azacytidine-treated hMSCs were co-cultured with fetal cardiomyocytes *in vitro*.

Result The established hMSCs proliferated over 150 population doublings. On day 3 of co-cultivation, the hMSCs became elongated, like myotubes, began spontaneously beating, and acquired automaticity. Their rhythm clearly differed from that of the surrounding fetal mouse cardiomyocytes. The number of beating cardiomyocytes increased until 3 weeks. hMSCs clearly exhibited differentiated cardiomyocyte phenotypes *in vitro* as revealed by immunocytochemistry, RT-PCR, and action potential recording.

Conclusions The life span of hMSCs was prolonged without interfering with cardiomyogenic differentiation. hMSCs with an extended life span can be used to produce a good experimental model of cardiac cell transplantation and may serve as a highly useful cell source for cardiomyocytic transplantation.

Keywords Bmi-1; marrow stroma; cardiomyocytes; immortalization; papillomavirus; senescence

Introduction

Cell transplantation has recently been attempted to improve cardiac function in severe heart failure. Many types of cells, such as embryonic stem cells [1,2], fetal cardiomyocytes [3–5], myoblasts [6,7], bone marrow hematopoietic cells [8,9], and mesenchymal stem cells (MSCs) [10–12], have been transplanted to functionally restore damaged or diseased tissue in animal models, and mononuclear cells [13–16] or myoblasts [17] have been injected into ischemic hearts clinically.

MSCs can be a useful source of cells for transplantation for several reasons: they have the ability to proliferate and differentiate into mesodermal tissues, including heart, they entail no ethical or immunological problems, and bone marrow aspiration is an established routine procedure. When placed in appropriate *in vitro* and *in vivo* environments, MSCs can give rise to all major mesenchymal tissues, such as bone, cartilage, muscle, and adipose tissue [18]. Murine MSCs can also differentiate into cardiomyocytes and start to beat synchronously *in vitro* [19], and direct injection of murine MSCs into the heart has been shown to be feasible in murine models of ischemic heart disease and normal mouse heart. Thus far, only endothelial cells have been shown to exhibit '*in vitro* cardiomyogenesis' in humans [20].

Large numbers of cells must be injected into damaged sites in ischemic heart disease to restore cardiac function in humans, and cells need to be injected into the entire heart in cardiomyopathy. Until now, however, there have been no reports of a sufficient number of differentiated human cardiomyocytes ever having been obtained to restore the function of a failing heart. One of the reasons for this is that the life span of human cells *in vitro* is limited. Human cells reach senescence or stop cell growth after a limited number of cell replications [21], and the average number of hMSC population doublings (PDs) has been found to be 38 [22], implying that it would be difficult to obtain enough cells to restore the function of a failing human heart.

To resolve these problems and to establish a model of cell therapy of the failing heart, we attempted to prolong the life span of hMSCs by using the system to infect retrovirus encoding bmi-1, human telomerase reverse transcriptase (TERT), and human papillomavirus E6 and E7 genes. Both Rb/p16INK4a inactivation with E7 and telomerase activation with E6 are required to extend the life span of human epithelial cells [23]. bmi-1, a c-myc cooperating oncogene in murine lymphomas, reduces expression of p16INK4a, stimulates cell proliferation [24], and is required for maintenance of self-renewing hematopoietic stem cells [25,26]. This method was highly efficient in extending the life span of hMSCs. In the present study we investigated whether hMSCs with an extended life span have the ability to differentiate into cardiomyocytes *in vitro*.

Materials and methods

Isolation and cell culture of hMSCs

After obtaining signed informed consent, bone marrow cells were harvested from a 91-year-old human female donor with the approval of the Ethics Committee of Keio University School of Medicine (Tokyo). Cells were resuspended in bone marrow stromal cell culture medium (10% fetal bovine serum in Dulbecco's modified Eagle's medium containing 4.5 g/l glucose [DMEM-HG]) with antibiotic/antimycotic supplements (Gibco), and cultures were maintained at 37 °C in a humidified atmosphere containing 95% air and 5% CO_2. When the cultures reached subconfluence, the cells were harvested with 0.25% trypsin and 1 mM EDTA, and replated with one half of the harvested cells. After a series of passages, the attached marrow stromal cells were devoid of hematopoietic cells. Several bone marrow stromal cell strains were then generated by the limiting-dilution method, and one of them was designated H4-1. The H4-1 cells were cultured in MSC growth medium (MSCGM) at 37 °C in a humidified atmosphere containing 95% air and 5% CO_2.

Preparation and infection of recombinant retroviruses

The full-length human bmi-1 cDNA was cloned by RT-PCR using RNA extracted from K562 cells. Thermoscript reverse transcriptase (Invitrogen) and KOD polymerase (TOYOBO, Japan) were used for the RT and PCR reactions, respectively. The forward primer, 5'-ACGCGTCGACCGCCATGCATCGAACAACGAGAAT-3', and reverse primer, 5'-CGGATCCTCAACCAGAAGAAGTTGCTG-3', were designed to obtain the coding sequence of human bmi-1 flanked by the *Sal*I site (underlined) and the Kozak consensus sequence at the 5'-end and the *Bam*HI site (underlined) at the 3'-end. The *Sal*I-*Bam*HI segment of the PCR product was cloned between the *Xho*I and *Bgl*II sites of pCLXSN to generate pCLXSN-bmi1. The coding sequence of the cDNA was confirmed to be identical to the published sequence (NCBI ACC# NM_005 180.4). Construction of pCLXSH-hTERT has been described previously [27]. The gateway system (Invitrogen) was used to subclone a deletion mutant of HPV16 E6 (16E6SDD151) that lacked transforming activity to 3Y1 cells [28] into pCMSCVpuro. pCMSCVpuro comprises the CMV/LTR fusion promoter, the packaging signal Psi, and the multicloning sequence from pCLXSN (Imgenex Corp., San Diego, CA, USA) followed by the PGK-puro cassette and the 3' long terminal repeat of murine embryonic stem cell virus from pMSCVpuro (Clontech). The destination vector pCMSCVpuro-DEST was constructed by inserting a modified cassette containing attR sites and ccdB (Invitrogen) between the *Eco*RI and *Bgl*II sites of pCMSCVpuro. 16E6SDD151 was first recombined into pDONR201 by BP reaction, and then into the destination vector by LR reaction according to the manufacturer's instructions (Invitrogen) to generate pCMSCVpuro-16E6SDD151. Production of recombinant retroviruses has been described previously [29,30]. Briefly, the retroviral vector together with the packaging construct, pCL-10A1, was transfected into 293T cells, and the culture fluid was harvested 48–72 h post-transfection. The preparation of the LXSN-16E7 retrovirus and the infection protocols have been described previously [31], except that FLYA13 [32] was used as the packaging cell line instead of PG13. The titers of the recombinant viruses were greater than 5×10^5 drug-resistant colony-forming units per milliliter on HeLa

cells, and 1 ml of the culture fluid was added to the cells in the presence of polybrene (8 μg/ml). Following inoculation with the viruses, hMSCs were grown in the presence of G418 (100 μg/ml), hygromycin B (50 μg/ml), or puromycin (1 μg/ml), and a polyclonal drug-resistant cell line was established and further analyzed. To achieve combinations of retroviral infections, cells were sequentially transduced with LXSN-E7 or LXSN-bmi-1, and LXSH-hTERT, and then MSCVpuro-16E6SDD151, if indicated, and selected with G418, hygromycin B, and puromycin, respectively. The stably transduced cells with an expanded life span were designated UBT-5, UBET-7, UEET-1, UEET-11, and UET-13.

Flow cytometric analysis

Cells were detached and stained for 30 min at 4 °C with primary antibodies and immunofluorescent secondary antibodies. After washing, the cells were analyzed on an EPICS ALTRA analyzer (Beckman Coulter). Antibodies (anti-human CD13, CD14, CD24, CD29, CD31, CD34, CD44, CD45, CD50, CD54, CD55, CD59, CD90, CD105, CD117, CD133, CD140a, CD166, Flk-1) were purchased from Beckman Coulter, Immunotech, Cytotech, and Pharmingen Pharmaceutical, Inc.

Introduction of the GFP and β-galactosidase genes

Recombinant adenovirus expressing β-galactosidase and the green fluorescent protein (GFP) was prepared as described [33]. Cells were infected with these viruses at 10 plaque-forming units/cell. hMSCs were examined cytochemically *in vitro* for expression of the β-galactosidase gene and by fluorescent confocal microscopy for expression of the GFP gene. By 7 days post-infection nearly all the cells expressed β-galactosidase and GFP.

Preparation of murine fetal cardiomyocytes

Fetal cardiomyocytes were obtained from the hearts of day 14 mouse fetuses. Hearts were minced with scissors and washed with phosphate-buffered saline (PBS), and the minced hearts were incubated in PBS with 0.05% trypsin and 0.25 mM EDTA for 5 min at 37 °C. After adding DMEM supplemented with 10% fetal bovine serum (FBS), the cardiomyocytes were centrifuged at 1000 rpm for 5 min. The pellet was then resuspended in 10 ml DMEM with 10% FBS and incubated on glass dishes for 1 h to separate the cardiomyocytes from fibroblasts. The floating cardiomyocytes were collected and replated at $1 \times 10^5/cm^2$.

hMSC and murine fetal cardiomyocyte co-culture system

Human MSCs were plated on dishes at $5 \times 10^4/cm^2$, and infected with EGFP-expressing adenovirus on the next day. The supernatant was then removed, and the cells were cultured for 2 days in DMEM supplemented with 10% FBS. The cells were then exposed to 10 μM of 5-azacytidine for 24 h to induce cell differentiation. The 5-azacytidine-treated hMSCs were harvested with 0.25% trypsin and 1 mM EDTA and overlaid onto the fetal cardiomyocytes at $5 \times 10^3/cm^2$. The morphology of the beating hMSCs was evaluated under a fluorescent microscope.

RT-PCR

Total RNA was prepared from co-cultured hMSCs and mouse heart with Isogen (Nippon Gene). Human cardiac RNA was purchased (Clontech). RNA for RT-PCR was converted to cDNA with a first-strand cDNA synthesis kit (Amersham Pharmacia Biotec) according to the manufacturer's recommendations. RT-PCR of the bmi-1, E6, E7, TERT, myosin light chain-2a (MLC-2a), Nkx2.5, and human atrial natriuretic peptide (hANP) genes was performed, and the PCR primers used are listed in Table 1. RT-PCR was performed with PCR primers that can amplify human but not mouse genes. PCR primers of 18S used as a positive control react with both human and murine genes. PCR was performed with TaKaRa Z-Taq (Takara Shuzo Co., Ltd) for 30 cycles, with each cycle consisting of 98 °C for 5 s, 68 °C or 60 °C for 1 s, and 72 °C for 10 s, with an additional 30-s incubation at 72 °C after completion of the final cycle.

Action potential recording and microinjection of dye

An inverted microscope (IX-70, Olympus, Tokyo, Japan) with a fluorescence filter (U-MNIBA2, Olympus) was used for action potential (AP) recording. The microscope was equipped with a recording chamber and a noise-free heating plate (Microwarm Plate, Kitazato Supply, Fujinomiya, Shizuoka, Japan). A 10 mmol/l volume of HEPES was added to the culture medium to stabilize the pH of the perfusate at 7.5–7.6. Standard glass microelectrodes having a DC resistance of 25–35 MΩ when filled with pipette solution were used. Alexa 568 compound was dissolved to a concentration of 0.5 mmol/l in 2 mol/l of KCl solution in order to completely dissolve the Alexa 568 in the pipette solution. The electrodes were positioned with a motor-driven micromanipulator (PCS-5000, Burleigh Instruments, Inc., New York, USA) under optical control. Spontaneously beating GFP-positive cells were selected as targets, and, after the APs of the targeted cells had been recorded, the dye was injected by iontophoresis (−7 nA for 30–60 s). The extent

Table 1. PCR primers used in this study

Gene product	Primer (sense)	Primer (anti-sense)	Annealing temperature (°C)	Product size (bp)
Bmi-1	TCATCCTTCTGCTGATGCTG	GCATCACAGTCATTGCTGCT	60	220
E6	GACCCAGAAAGTTACCACAG	GCAACAAGACATACATCGAC	60	397
E7	ATGACAGCTCAGAGGAGGAG	TCCTAGTGTGCCCATTAACAG	60	178
TERT	CGGAAGAGTGTCTGGAGCAA	GGATGAAGCGGAGTCTGGA	60	144
MLC-2a				
1st	TCGTGATGGCATCATCTGCAAGG	ACAGAGTTTATTGAGGTGCCCC	60	429
2nd	AAGGTGAGTGTCCCAGAGG	ATGGGTGTCAGGGCGAACATC	60	259
NkX2.5				
1st	CTTCAAGCCAGAGGCCTACG	CCGCCTCTGTCTTCTCCAGC	60	233
2nd	CTTCACCGGCCAAGTGTGCGTC	CCGCCTCTGTCTTCTCCAGC	60	152
hANP				
1st	GAACCAGAGGGGAGAGACAGAG	CCCTCAGCTTGCTTTTTAGGAG	60	406
2nd	GTCAGACCAGAGCTAATCCC	ACCTCCATCTCTCTGGGCTG	68	223
18S	GTGGAGCGATTTGTCTGGTT	CGCTGAGCCAGTCAGTGTAG	60	200

of dye transfer was monitored under a fluorescence microscope, and digital images were recorded with a digital photo camera (D100; Nikon, Tokyo, Japan) mounted on the microscope with a fluorescence filter (U-MWIG2; Olympus). The recording pipette was connected to a patch-clamp amplifier (Axopatch 200B; Axon Instruments), and the signal was low-pass filtered at 2 kHz and digitized with an A/D converter with sampling frequency of 10 kHz (Digidata 1322A; Axon Instruments) connected to a computer with Pentium4. Signals were monitored, recorded as electric files, and analyzed offline with pCLAMP 8.2 software (Axon Instruments). The rhythm was considered regular if the maximum beating rate minus the minimum beating rate divided by the max beating rate was <0.4.

Immunohistochemistry

The hMSCs co-cultured with fetal cardiomyocytes *in vitro* were fixed with 4% PFA and stained with anti-β2microglobulin antibody at 1 : 1000, mouse monoclonal antibody against troponin I (Hytest, Euro, Finland) at 1 : 200, anti-desmin antibody at 1 : 100, and anti-β-galactosidase antibody (Chemicon) at 1 : 500. hMSCs expressing GFP were fixed with 4% PFA.

Results

Establishment of hMSCs with an extended life span

H4-1 cells were obtained from primary culture by limiting dilution (Figure 1A). The cells proliferated for a limited number of passages and then underwent senescence, as evidenced by the cells assuming a broad and flattened shape (Figures 1B and 1C). To extend the life span of H4-1 cells, and obtain a large number of cells for cardiac transplantation, four different types of cells were obtained by transferring combinations of bmi-1, E6, E7, and/or TERT genes. Cells transduced with bmi-1 and TERT were designated UBT-5 cells; cells transduced with bmi-1, E6, and TERT were named UBET-7 cells; cells transduced with E7 and TERT were designated UET-13 cells; and cells transduced with E6, E7, and TERT were named UEET-1 and UEET-11 cells (Figures 1D, 1E, and 1F). To simplify nomenclature and avoid confusion, we use the name UEET-1 to refer to cells transduced with E6, E7, and TERT although they have recently been reported as ThMSC1 [29]. The cells were subcloned after each gene transfer, and thus were clonal. The UEET-1 cells were spindle-shaped, and longer than the parental H4-1 cells (Figures 1B, 1D, and 1E). Characteristics of cells with a prolonged life span were investigated. UEET-11 and UET-13 proliferated more than 150 PDs in 400 days, and UBET-7 and UBT-5 proliferated more than 50 PDs in 400 days, while H4-1 stopped dividing at 38 PDs (approximately 200 days). The growth rates of UEET-11 and UET-13 were higher than those of UBT-5 and UBET-7. Chromosome analysis revealed parental H4-1 and UET-13 to exhibit normal karyotypes, while the other cells transduced with E6 and E7 showed chromosome aberrations at low frequencies (data not shown). The transduced cells did not generate tumors, at least for the first 60 days after subcutaneous transplantation into immunodeficient mice.

Surface analysis of hMSCs

Surface markers of the UEET-1, UEET-11, UBT-5, UBET-7, and UET-13 cells were evaluated by flow cytometric analysis. The results showed that all of the MSCs were positive for CD13, CD29 (integrin β1), CD44 (Pgp-1/ly-24), CD55, CD59, CD90 (Thy-1), CD105 (endoglin), CD133, CD140a (PDGFRα or PDGFR2), and CD166 (ALCAM), and negative for CD14 (a marker for macrophage and dendritic cells), CD24, CD31 (PECAM-1), CD34, CD45 (leukocyte common antigen), CD50 (ICAM-3), CD54, CD117 (c-kit), and Flk-1 (Figure 2). Parental H4-1 cells had the same pattern of surface markers as UEET-1, UEET-11, UBT-5, and UBET-7 cells, implying that the surface markers were not influenced by

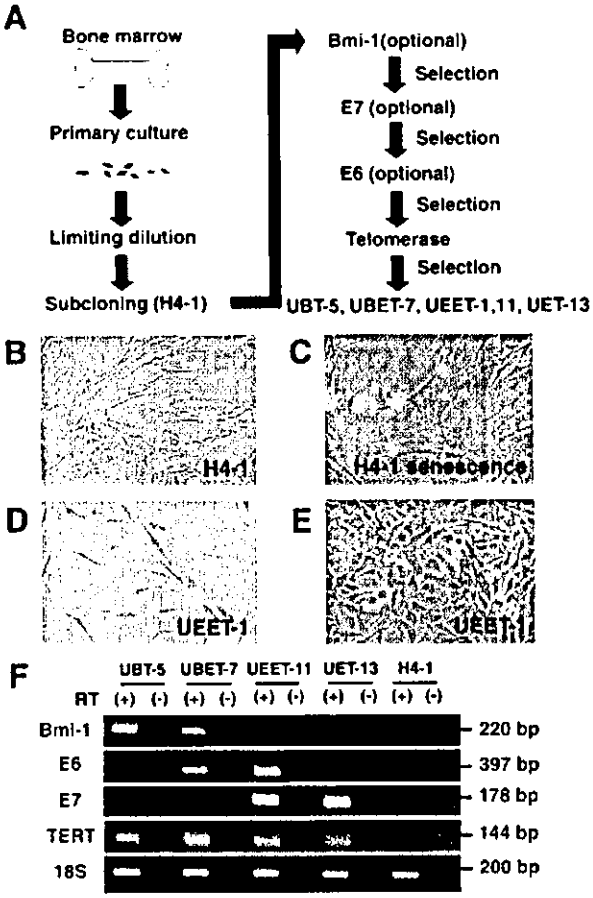

Figure 1. Experimental scheme. (A) Bone marrow stromal cells were obtained from a human donor and subcloned by limiting dilution. One of the cells isolated was designated H4-1 cells, and they were transduced with E6, E7, TERT, or bmi-1 genes to extend their life span. The combinations of genes transferred were: (1) bmi-1 and TERT; (2) bmi-1, E7, and TERT; (3) E7 and TERT; and (4) E6, E7, and TERT. (B) H4-1 cells in the growth phase. (C) H4-1 cells at senescence. The cells showed a broad and flattened shape. (D) H4-1 cells after transfer of E6, E7, and TERT genes were designated UEET-1 cells. (E) UEET-1 cells at confluence. Original magnification, B–E: ×100. (F) The gene expression in each cell line was analyzed using RT-PCR

the exogeneously expressed bmi-1, E6, E7, and/or TERT genes.

Cardiomyogenic differentiation of hMSCs and stably transduced hMSCs

To determine whether H4-1 cells could be induced to undergo cardiomyogenic differentiation, the cells were exposed to 10 μM of 5-azacytidine for 24 h as previously reported in murine stromal cells [19]. All of the transduced hMSCs did not exhibit spontaneous beating despite continuous culturing for up to 3 months. Immunocytochemical analysis revealed the presence of desmin, a myocytic marker, in the hMSCs with an extended life span, i.e., UBT-5 cells and UBET-7 cells (Figure 3A). However, all cells tested were negative for the cardiomyocyte marker troponin-I (Figure 3B).

We employed a co-culture system with fetal cardiomyocytes to induce cardiac differentiation (Figure 4), since *in vitro* simulation of the heart by the environment has been shown to be an efficient means of induced differentiation of human endothelial progenitor cells and murine marrow stromal cells [20,34]. After exposing GFP-labeled UBT-5, UBET-7, UEET-11, and UET-13 cells to 10 μM of 5-azacytidine for 24 h, these cells were co-cultured with fetal cardiomyocytes. On day 3 after the start of co-cultivation, a few GFP-positive UBET-7 cells started to contract (Figure 5A). The contraction was stronger when beating cells were clustered than when scattered (Figure 5B). On day 7, the beating of the UBET-7 cells was synchronous with that of adjacent cells and was independent of that of the surrounding murine cardiomyocytes (Figures 5C and 5D). Repetition of these experiments confirmed the results to be reproducible, and the percentages of UBT-5, UBET-7, UEET-11, and UET-13 cells that underwent cardiomyogenic differentiation were almost the same, implying that cardiomyogenic differentiation is independent of the genes transferred. The number of beating cells increased for up to 3–4 weeks, when the fetal cardiomyocytes spontaneously detached from the dishes (Figure 5E). UBET-7 cells not treated with 5-azacytidine were co-cultured with fetal cardiomyocytes to determine whether environmental factors alone can induce cardiac differentiation, but fewer beating cells were observed (Figure 5F). No significant difference was detected in the number of differentiated cells between parental H4-1 and UBET-7 (Figure 5G).

Expression of cardiomyocyte-specific genes and proteins and the action potential of differentiated hMSCs

We analyzed the co-cultured UBET-7 cells in terms of gene expression and by immunocytochemistry and electrical recording. RT-PCR was performed with primers that react with human cardiomyocyte-specific genes but not with murine orthologues. Differentiated UBET-7 cells expressed MLC-2a, hANP, and the cardiomyocyte-specific transcription factor, Nkx2.5/Csx (Figure 6). Sequence analysis revealed that the cDNAs matched the sequences of the human MLC-2a, hANP, and Nkx2.5/Csx genes.

Action potentials were recorded from spontaneously beating cells. Alexa 568 was injected into cells via a recording microelectrode to stain the cells and confirm that the action potential was generated by GFP-positive UBET-7 cells (Figures 7A and 7B). Since the dye did not diffuse into the murine cardiomyocytes, there were no tight cell-to-cell heterologous connections, i.e., gap junctions. In some experiments, Alexa 568 diffused into the GFP-positive satellite UBET-7 cells, suggesting that a homologous cell-to-cell connection had been established at least 1 week after co-cultivation. The measured parameters of the recorded action potential were averaged

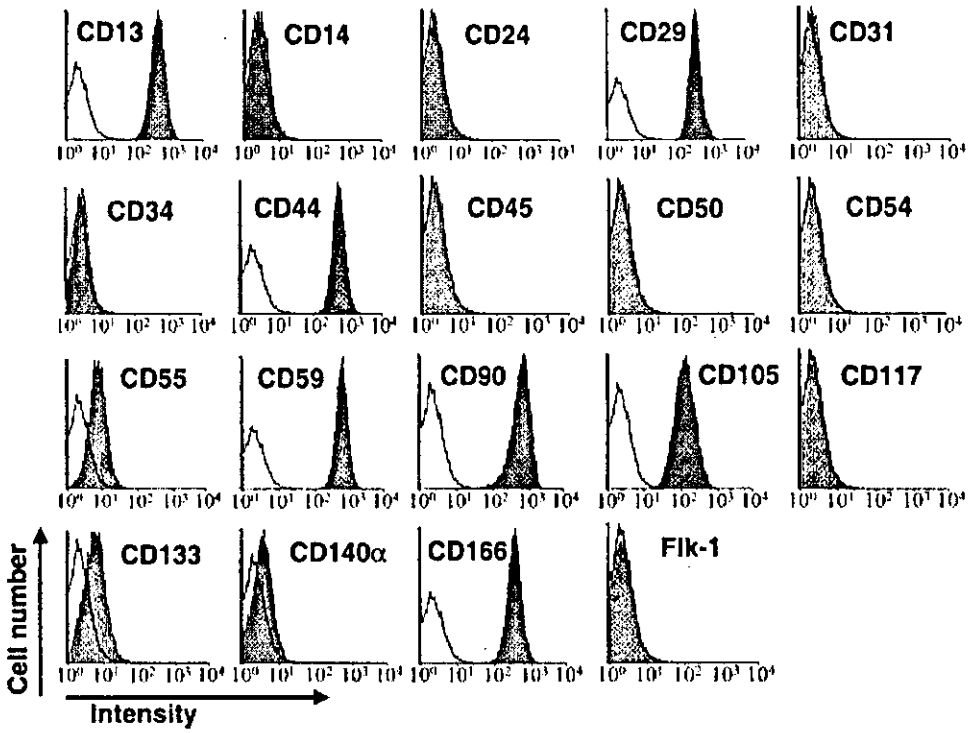

Figure 2. Flow cytometric analysis of UEET-1 cells. UEET-1 cells were labeled with FITC-coupled antibodies against CD13, CD14, CD24, CD29, CD31, CD34, CD44, CD45, CD50, CD54, CD55, CD59, CD90, CD105, CD117, CD133, CD140a, CD166, and Flk-1 and analyzed with an EPICS ALTRA analyzer

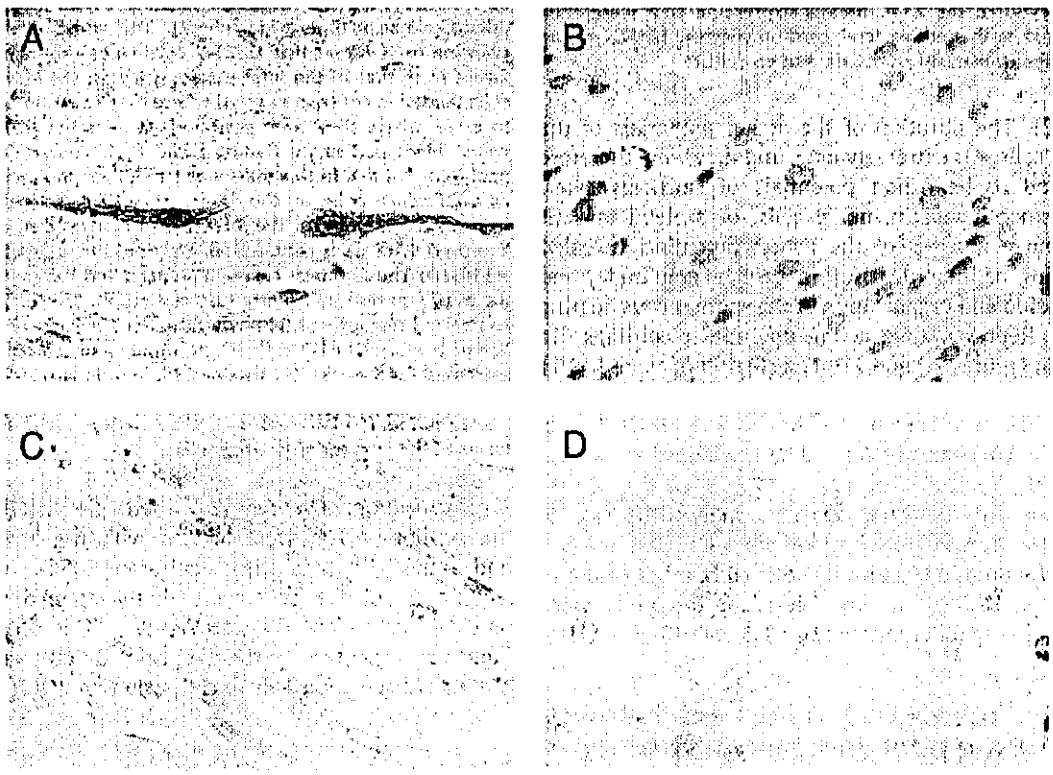

Figure 3. Immunostaining of hMSCs with anti-desmin and anti-troponin-I antibodies after exposure to 5-azacytidine. UBET-7 cells were exposed to 10 μM of 5-azacytidine for 24 h and stained for desmin (A) and cardiac troponin I (B). UBET-7 cells not treated with 5-azacytidine were also stained for desmin (C) and cardiac troponin I (D). Original magnification: ×400

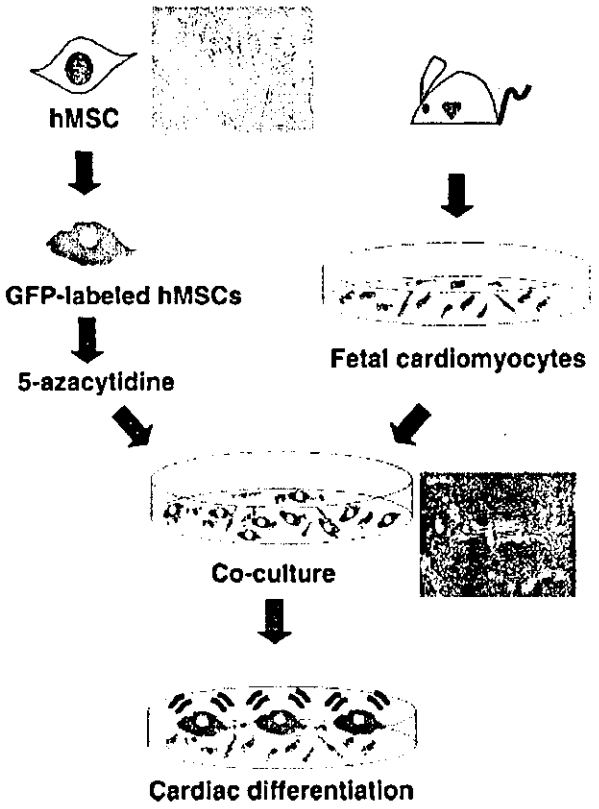

Figure 4. Scheme of the co-culture system. hMSCs infected with adenoviruses carrying the GFP gene were treated with 10 μM of 5-azacytidine for 24 h. hMSCs expressing GFP were then co-cultured with murine fetal cardiomyocytes. hMSCs began beating spontaneously after 7 days of co-culture

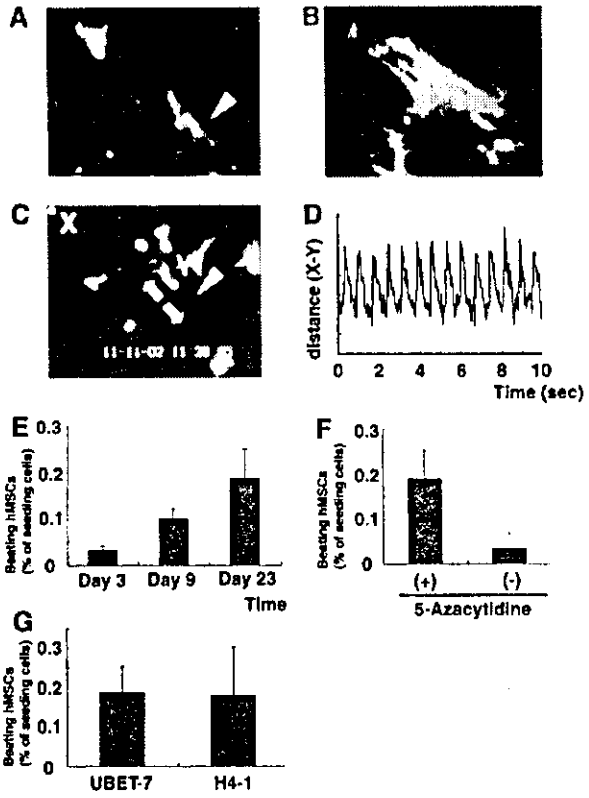

Figure 5. Beating of hMSCs in the *in vitro* co-culture system. (A) 5-Azacytidine-treated GFP-positive UBET-7 cells were co-cultured with murine fetal cardiomyocytes (http://1985.jukuin.keio.ac.jp/umeza/jgm/ubet7). The white arrowhead is pointing to some beating UBET-7 cells whose rhythm was different from that of the fetal cardiomyocytes. (B) More UBET-7 cells tended to contract in areas where they were clustered than in areas where they were scattered. (C) Beating UBET-7 cells were videotaped at 30 flames/s and their contractions were analyzed. Point X in this view was fixed, and point Y was used as a reference point on the differentiated UBET-7 cell (arrowhead). Arrows point in the direction of contraction, and point Y moved with each contraction. Original magnification, A–C: ×150. (D) The distances between points X and Y were measured for a 10-s period and plotted on the graph. The UBET-7 cells contracted regularly at 84 beats/min. (E) The ratio of the number of beating UBET-7 cells to the number of the cells seeded increased for 3 weeks. (F) On day 23, the ratio was higher in the cells exposed to 5-azacytidine than in the cells not exposed to 5-azacytidine. (G) Parental H4-1 was compared with UBET-7 in terms of the number of beating cells

(Table 2). The duration of the action potentials of the UBET-7 cells was extremely long, and they were therefore concluded to be action potentials of cardiomyocytes, not of smooth muscle, nerve cells, or skeletal muscle. Time-course analysis of the action potentials revealed shortening of their duration, a gain in amplitude, and stabilization and organization of the spontaneous beating rhythm. Representative action potential recordings are shown in Figures 7C and 7D. The rhythm of some (33%) of the UBET-7 cells was still disorganized at 1 week (Figure 7C), whereas the rhythm of the UBET-7 cells (100%) had become regular and had stabilized at 3 weeks (Figure 7D).

Immunohistochemistry revealed that UBET-7 cells expressing human β2microglobulin and GFP stained positive for desmin (Figures 8A–8C) and cardiac troponin I (Figures 8D–8F) on day 14. Clear striations were observed in the differentiated UBET-7 cells (Figure 8H).

Absence of cell fusion between hMSCs and murine fetal cardiomyocytes

To determine whether the beating cells had fused with the fetal cardiomyocytes, GFP-expressing hMSCs were co-cultured with fetal cardiomyocytes labeled with β-galactosidase. On day 7, when almost 100% of the cardiomyocytes were labeled with β-galactosidase, and almost 100% of the co-cultured-hMSCs expressed GFP, none of the cells were double-stained for GFP and β-galactosidase (Figures 9A–9D). This observation indicates that the cardiomyogenic differentiation of hMSCs is not attributable to cell fusion on day 7.

Discussion

This study was conducted to determine whether prolongation of cell life span by cell-cycle-associated molecules

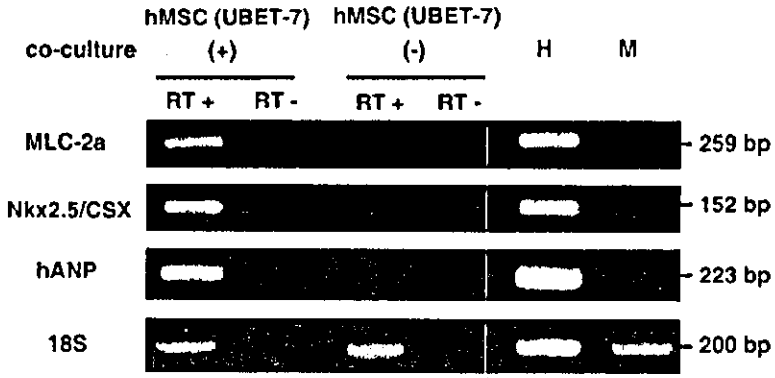

Figure 6. Expression of cardiomyocyte-specific genes in differentiated hMSCs (UBET-7). RT-PCR was performed with PCR primers that react with human genes encoding cardiac proteins (MLC-2a, Nkx2.5, and hANP) but do not with the murine genes. Only the 18S PCR primer used as a positive control reacted with the human and murine genes. Human heart (H) and mouse heart (M) were used as a positive control and negative control, respectively. The human cardiac genes, MLC-2a, Nkx2.5/csx and hANP, were expressed in the co-culturing system, but were not expressed in the undifferentiated state (without feeder cells)

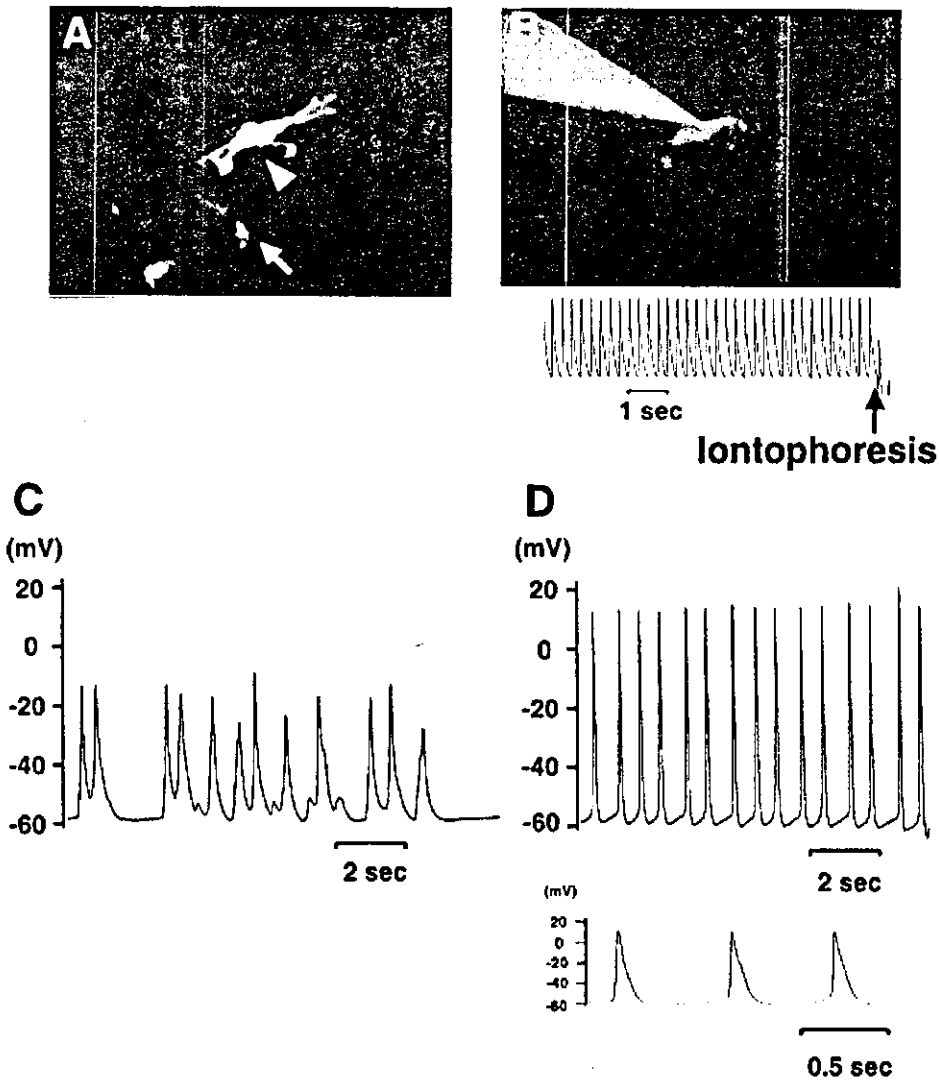

Figure 7. Action potentials of beating hMSCs. GFP-labeled UBET-7 cells (A) were injected with Alexa 568 solution (B) by iontophoresis through a microelectrode. The injected UBET-7 cell and neighboring beating UBET-7 cell are indicated by arrowhead and arrow, respectively. The action potential was recorded (B, lower panel). Some of the rhythms recorded at 1 week of co-cultivation were irregular (C), but the rhythm became regular at 3 weeks (D); top: large scale (2 s), bottom: small scale (0.5 s). Original magnification, A, B: ×400

Table 2. Action potential parameters in human mesenchymal stem cell derived cardiomyocytes

Time of co-culture	n	Ratio of regular rate	Beating rate (beats/min)	MDP (mV)	Amplitude (mV)	APD_{90} (ms)
1 week	12	67%	70.6 ± 12.8	−49.9 ± 1.6	47.2 ± 2.9	345.8 ± 21.4
2 weeks	9	67%	65.9 ± 12.7	−50.3 ± 2.3	60.2 ± 4.5	169.7 ± 13.8
3 weeks	9	100%	68.2 ± 12.1	−45.1 ± 1.4	63.7 ± 3.0	163.4 ± 16.5

The values are shown as mean ± S.E. The ratio of regular rate: regular beating rhythm/irregular beating rhythm. MDP: maximum diastolic potential. APD: action potential duration.

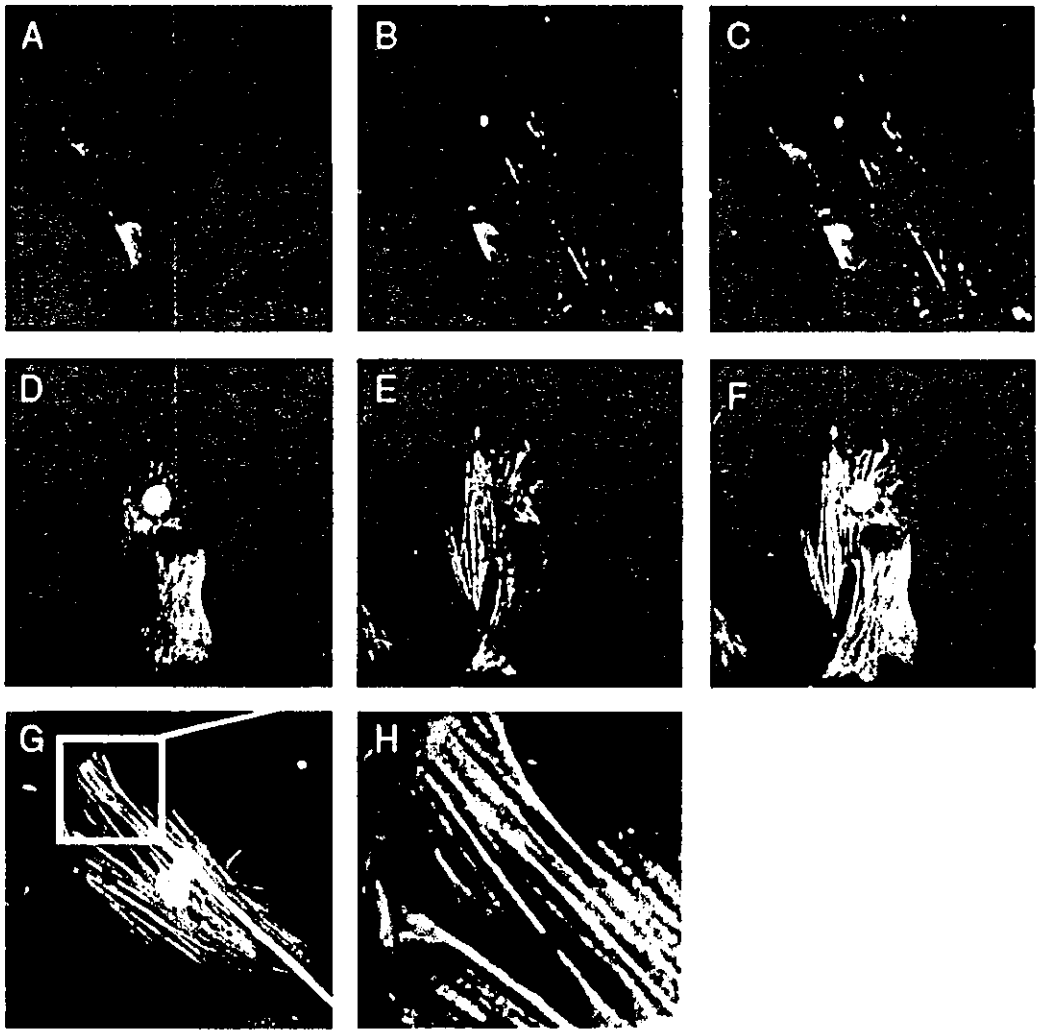

Figure 8. Immunocytochemistry of differentiated hMSCs with anti-desmin and anti-troponin-I antibodies. UBET-7 cells were co-cultured with cardiomyocytes. UBET-7 cells were analyzed for myogenic and cardiac differentiation by immunohistochemistry with desmin and cardiac troponin-I, respectively. Co-cultured UBET-7 cells were stained with anti-β2microglobulin antibody (A) and anti-desmin antibody (B). A superimposed image ('Merge') of A and B is shown in C. GFP-expressing UBET-7 cells (D) were stained with anti-troponin-I antibody (E). 'Merge' is shown in F. A differentiated UBET-7 cell is shown at higher magnification (G). The differentiated UBET-7 cells have striations in their cytoplasm (H). Original magnification, A–G: ×600, H: ×2000

would predominate over cardiomyogenic differentiation of marrow stromal cells *in vitro*. The primary findings of the present study were: (1) the life span of hMSCs was extended by bmi-1, E6, E7, and TERT; (2) hMSCs exposed to 5-azacytidine and cultured with fetal cardiomyocytes underwent cardiomyogenic differentiation as manifested by their morphology, gene expression, and electrophysiology, and started to beat spontaneously (automaticity); and (3) cardiomyogenic differentiation of the hMSCs was not attributable to cell fusion.

MSCs are pluripotent cells capable of differentiating into many cell types, such as neurons [35], myocytes, cardiomyocytes, chondrocytes, and adipocytes [36]. Multipotent adult progenitor cells (MAPCs) have recently

Table 2. Action potential parameters in human mesenchymal stem cell derived cardiomyocytes

Time of co-culture	n	Ratio of regular rate	Beating rate (beats/min)	MDP (mV)	Amplitude (mV)	APD_{90} (ms)
1 week	12	67%	70.6 ± 12.8	−49.9 ± 1.6	47.2 ± 2.9	345.8 ± 21.4
2 weeks	9	67%	65.9 ± 12.7	−50.3 ± 2.3	60.2 ± 4.5	169.7 ± 13.8
3 weeks	9	100%	68.2 ± 12.1	−45.1 ± 1.4	63.7 ± 3.0	163.4 ± 16.5

The values are shown as mean ± S.E. The ratio of regular rate: regular beating rhythm/irregular beating rhythm. MDP: maximum diastolic potential. APD: action potential duration.

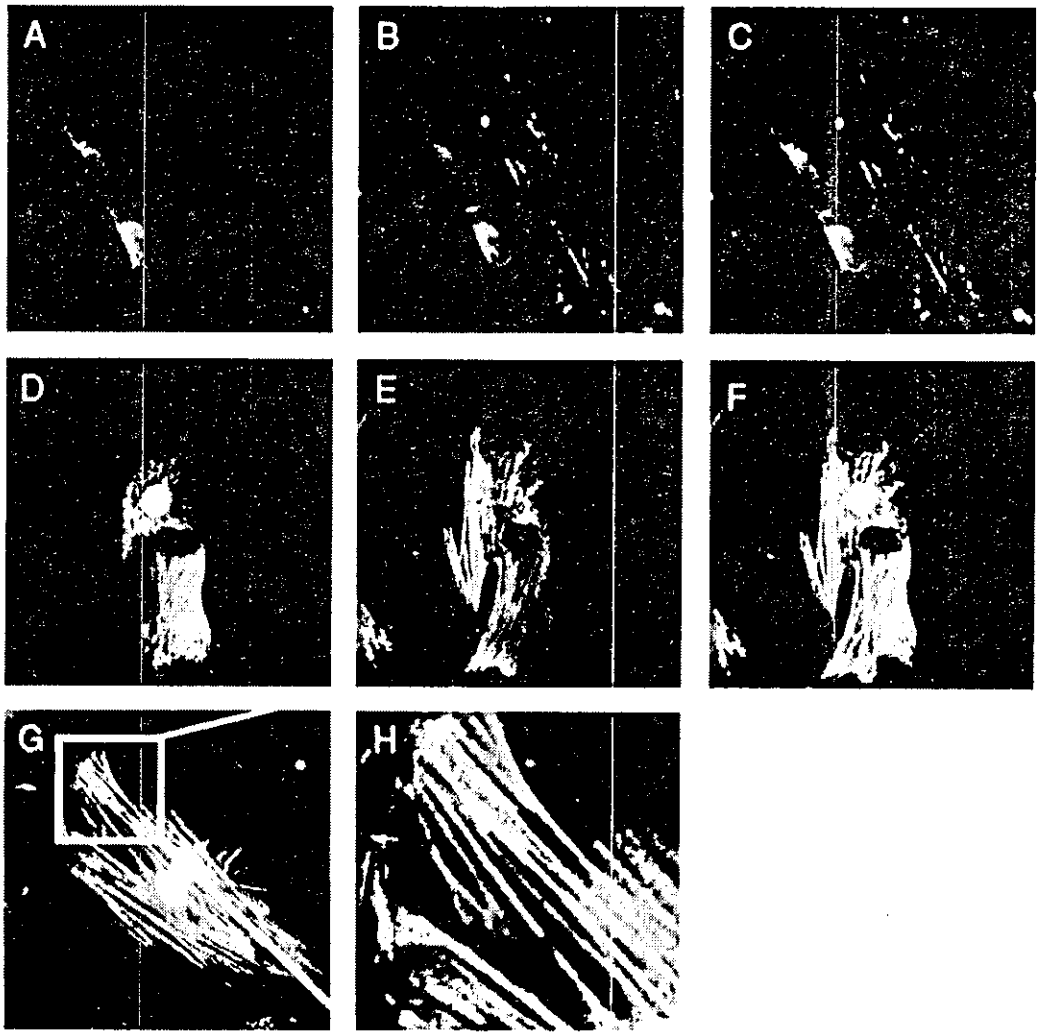

Figure 8. Immunocytochemistry of differentiated hMSCs with anti-desmin and anti-troponin-I antibodies. UBET-7 cells were co-cultured with cardiomyocytes. UBET-7 cells were analyzed for myogenic and cardiac differentiation by immunohistochemistry with desmin and cardiac troponin-I, respectively. Co-cultured UBET-7 cells were stained with anti-β2microglobulin antibody (A) and anti-desmin antibody (B). A superimposed image ('Merge') of A and B is shown in C. GFP-expressing UBET-7 cells (D) were stained with anti-troponin-I antibody (E). 'Merge' is shown in F. A differentiated UBET-7 cell is shown at higher magnification (G). The differentiated UBET-7 cells have striations in their cytoplasm (H). Original magnification, A–G: ×600, H: ×2000

would predominate over cardiomyogenic differentiation of marrow stromal cells *in vitro*. The primary findings of the present study were: (1) the life span of hMSCs was extended by bmi-1, E6, E7, and TERT; (2) hMSCs exposed to 5-azacytidine and cultured with fetal cardiomyocytes underwent cardiomyogenic differentiation as manifested by their morphology, gene expression, and electrophysiology, and started to beat spontaneously (automaticity); and (3) cardiomyogenic differentiation of the hMSCs was not attributable to cell fusion.

MSCs are pluripotent cells capable of differentiating into many cell types, such as neurons [35], myocytes, cardiomyocytes, chondrocytes, and adipocytes [36]. Multipotent adult progenitor cells (MAPCs) have recently

is incorporated into DNA and has been shown to cause extensive demethylation. The demethylation is attributable to covalent binding of DNA methyltransferase to 5-azacytidine in the DNA [42], with the subsequent reduction of enzyme activity in cells resulting in dilution-out and random loss of methylation at many sites in the genome. This may in turn account for the reactivation of cardiomyogenic 'master' genes, such as MEF-2C, GATA4, dHAND, and Nkx2.5/Csx, leading to stochastic transdifferentiation of MSCs into cardiomyocytes. Use of 5-azacytidine is beneficial, but since it may have drawbacks, i.e., gene activation leading to oncogenesis and undesired differentiation, care must be exercised before using it to simply induce cells to differentiate into target phenotype(s) because of its stochastic nature.

Thus, it may be necessary to find alternative humoral factors essential for cardiomyogenic differentiation to prepare cells for cell therapy in humans. In addition to demethylating agents, environmental factors promote cardiomyocyte differentiation. A co-culture system has recently been used to induce cardiac differentiation, and human endothelial progenitor cells have been found to transdifferentiate into cardiomyocytes with this system [20]. Murine MSCs have been shown to differentiate into a cardiomyogenic lineage [43], but to our knowledge the present study is the first to report spontaneous beating by human MSCs and exhibition of *'in vitro'* automaticity without cell fusion. These results simply imply that MSCs may have the ability to transdifferentiate into cardiomyocytes in response to demethylation of the genome, in addition to environmental factors.

Co-cultivation makes it difficult to investigate two different types of cells in detail because they are present on the same dishes, and the target cells are difficult to isolate. There was also the question of whether the presence of beating cells means differentiation to cardiomyocytes, or merely fusion with fetal cardiomyocytes. Since marrow cells spontaneously fuse with co-cultured ES cells *in vitro* [44], controversy has arisen as to whether regenerated myocardium represents transplanted cells fused with native cardiomyocytes instead of differentiated donor cells. Cell fusion did not occur in our study, however, because cardiomyogenic differentiation was demonstrated by the double-labeling of two types of co-cultured cells *in vitro*.

The co-culture of the target cells, i.e., the marrow stroma, in this study, on appropriate feeder cells may provide a good system for generating a source of cells for therapy. hMSCs have the ability to form tight cell-to-cell couplings, i.e., gap junctions, with adjacent hMSCs, suggesting that the grafted hMSCs are capable of generating electrical coupling and may function coordinately in the recipient human heart. On the other hand, the disorganization of the spontaneous beating rhythm in the early stage may result in arrhythmogenesis when grafted into the recipient. Early afterdepolarization, which triggers arrhythmias, has been reported in cardiomyocytes generated by ES cells or embryonal carcinoma cells [45]. By contrast, the absence of early afterdepolarization in hMSCs may be beneficial in terms of not leading to arrhythmias when the cells are transplanted *in vivo*. The rhythm of the hMSCs that underwent premature differentiation became regular after complete differentiation in the present study, and culture for a certain period therefore seems necessary before cell transplantation. It is noteworthy that the risk of lethal arrhythmia can be reduced by promoting electrical maturation of hMSCs *in vitro* when this co-culture system is used for therapy clinically.

It remains unresolved how co-cultured hMSCs start beating spontaneously and what the key factor(s) in cardiac differentiation are. Several factors promote differentiation into cardiomyocytes, such as gap junctions, humoral factors, electrical and mechanical stimulation, and cell-to-cell contact. Gap junctions have been shown to be necessary for differentiation of endothelial progenitor cells to cardiomyocytes [20], but the lack of gap junctional communication between hMSCs and feeder cells in our study indicates that gap junctions are not prerequisite for differentiation. In addition, separation of hMSCs and fetal cardiomyocytes in a co-culture system with a membrane that is permeable to humoral factors but not to cells resulted in loss of capacity for cardiac differentiation (data not shown), implying that humoral factors alone do not induce cardiac differentiation of hMSCs, and direct interactions, such as with cell-membrane bound molecules and extracellular matrix, seem to be essential. Cadherins, for example, have been reported to mediate calcium-dependent cell-to-cell contact and affect the differentiation of cardiac muscle cells [46]. Moreover, the decrease in number of beating hMSCs after the feeder cells stopped beating implies that mechanical stimulation in addition to cell-to-cell contact might be indispensable to cardiac differentiation and maintenance of the differentiated state.

Many clinical trials of regeneration therapy using mononuclear cells for the failing heart have been performed [13–16], but many more basic studies are needed. hMSCs with an expanded life span cannot be transplanted clinically, because they have been transduced with human papillomavirus E6 and E7 genes. The present results and others have shown that these molecules do not elicit cell transformation *in vitro*, at least during the period observed. This contrasts with human stromal cells being transformed during immortalization by SV40 large T antigen [47]. Based on the results of this study and the mechanism of cell life span extension, we are now developing a novel strategy to eliminate the possibility of transformation. Thus, cells that undergo reproducible cardiomyogenic differentiation and have a prolonged life span can be used as a good model of cell transplantation.

Acknowledgements

We would like to express our sincere thanks to K. Tsuchiya, T. Uyama and S. Matsumoto for support throughout the work, and T. Inomata, Y. Nakamura, and Y. Taki for providing expert

technical assistance. We are grateful to Dr. D. A. Galloway (FHCRC, Seattle, USA) for pLXSN-16E7 and to Dr. Y. Takeuchi (Chester Beatty Laboratories, ICR, UK) for the FLYA13 cells. This work was supported in part by a special grant for Advanced Research on Cancer from the Ministry of Education, Culture, Sports, Science, and Technology of Japan to T. K. and A. U., and the Organization for Pharmaceutical Safety and Research to A.U.

The cell names are summarized at http://1985.jukuin.keio.ac.jp/umezawa/cells/name.html. MPEG video stream of UBET-7 is available at http://1985.jukuin.keio.ac.jp/umezawa/jgm/ubet7.

References

1. Klug MG, Soonpaa MH, Koh GY, Field LJ. Genetically selected cardiomyocytes from differentiating embryonic stem cells form stable intracardiac grafts. *J Clin Invest* 1996; **98**: 216–224.
2. Min JY, Yang Y, Converso KL, *et al.* Transplantation of embryonic stem cells improves cardiac function in postinfarcted rats. *J Appl Physiol* 2002; **92**: 288–296.
3. Etzion S, Battler A, Barbash IM, *et al.* Influence of embryonic cardiomyocyte transplantation on the progression of heart failure in a rat model of extensive myocardial infarction. *J Mol Cell Cardiol* 2001; **33**: 1321–1330.
4. Muller-Ehmsen J, Whittaker P, Kloner RA, *et al.* Survival and development of neonatal rat cardiomyocytes transplanted into adult myocardium. *J Mol Cell Cardiol* 2002; **34**: 107–116.
5. Muller-Ehmsen J, Peterson KL, Kedes L, *et al.* Rebuilding a damaged heart: long-term survival of transplanted neonatal rat cardiomyocytes after myocardial infarction and effect on cardiac function. *Circulation* 2002; **105**: 1720–1726.
6. Ghostine S, Carrion C, Souza LC, *et al.* Long-term efficacy of myoblast transplantation on regional structure and function after myocardial infarction. *Circulation* 2002; **106**: I131–136.
7. Taylor DA, Atkins BZ, Hungspreugs P, *et al.* Regenerating functional myocardium: improved performance after skeletal myoblast transplantation. *Nat Med* 1998; **4**: 929–933.
8. Jackson KA, Majka SM, Wang H, *et al.* Regeneration of ischemic cardiac muscle and vascular endothelium by adult stem cells. *J Clin Invest* 2001; **107**: 1395–1402.
9. Orlic D, Kajstura J, Chimenti S, *et al.* Bone marrow cells regenerate infarcted myocardium. *Nature* 2001; **410**: 701–705.
10. Wang JS, Shum-Tim D, Galipeau J, Chedrawy E, Eliopoulos N, Chiu RC. Marrow stromal cells for cellular cardiomyoplasty: feasibility and potential clinical advantages. *J Thorac Cardiovasc Surg* 2000; **120**: 999–1005.
11. Shake JG, Gruber PJ, Baumgartner WA, *et al.* Mesenchymal stem cell implantation in a swine myocardial infarct model: engraftment and functional effects. *Ann Thorac Surg* 2002; **73**: 1919–1925; discussion 1926.
12. Gojo S, Gojo N, Takeda Y, *et al.* In vivo cardiovasculogenesis by direct injection of isolated adult mesenchymal stem cells. *Exp Cell Res* 2003; **288**: 51–59.
13. Strauer BE, Brehm M, Zeus T, *et al.* Repair of infarcted myocardium by autologous intracoronary mononuclear bone marrow cell transplantation in humans. *Circulation* 2002; **106**: 1913–1918.
14. Hamano K, Nishida M, Hirata K, *et al.* Local implantation of autologous bone marrow cells for therapeutic angiogenesis in patients with ischemic heart disease: clinical trial and preliminary results. *Jpn Circ J* 2001; **65**: 845–847.
15. Assmus B, Schachinger V, Teupe C, *et al.* Transplantation of progenitor cells and regeneration enhancement in acute myocardial infarction (TOPCARE-AMI). *Circulation* 2002; **106**: 3009–3017.
16. Tse HF, Kwong YL, Chan JK, Lo G, Ho CL, Lau CP. Angiogenesis in ischaemic myocardium by intramyocardial autologous bone marrow mononuclear cell implantation. *Lancet* 2003; **361**: 47–49.
17. Menasche P, Hagege AA, Scorsin M, *et al.* Myoblast transplantation for heart failure. *Lancet* 2001; **357**: 279–280.
18. Prockop DJ. Marrow stromal cells as stem cells for nonhematopoietic tissues. *Science* 1997; **276**: 71–74.
19. Makino S, Fukuda K, Miyoshi S, *et al.* Cardiomyocytes can be generated from marrow stromal cells in vitro. *J Clin Invest* 1999; **103**: 697–705.
20. Badorff C, Brandes RP, Popp R, *et al.* Transdifferentiation of blood-derived human adult endothelial progenitor cells into functionally active cardiomyocytes. *Circulation* 2003; **107**: 1024–1032.
21. Hayflick L, Moorhead PS. The serial cultivation of human diploid cell strains. *Exp Cell Res* 1961; **25**: 585–621.
22. Bruder SP, Jaiswal N, Haynesworth SE. Growth kinetics, self-renewal, and the osteogenic potential of purified human mesenchymal stem cells during extensive subcultivation and following cryopreservation. *J Cell Biochem* 1997; **64**: 278–294.
23. Kiyono T, Foster SA, Koop JI, McDougall JK, Galloway DA, Klingelhutz AJ. Both Rb/p16INK4a inactivation and telomerase activity are required to immortalize human epithelial cells. *Nature* 1998; **396**: 84–88.
24. Jacobs JJ, Kieboom K, Marino S, DePinho RA, van Lohuizen M. The oncogene and Polycomb-group gene bmi-1 regulates cell proliferation and senescence through the ink4a locus. *Nature* 1999; **397**: 164–168.
25. Lessard J, Sauvageau G. Bmi-1 determines the proliferative capacity of normal and leukaemic stem cells. *Nature* 2003; **423**: 255–260.
26. Park IK, Qian D, Kiel M, *et al.* Bmi-1 is required for maintenance of adult self-renewing haematopoietic stem cells. *Nature* 2003; **423**: 302–305.
27. Okamoto T, Aoyama T, Nakayama T, *et al.* Clonal heterogeneity in differentiation potential of immortalized human mesenchymal stem cells. *Biochem Biophys Res Commun* 2002; **295**: 354–361.
28. Kiyono T, Hiraiwa A, Fujita M, Hayashi Y, Akiyama T, Ishibashi M. Binding of high-risk human papillomavirus E6 oncoproteins to the human homologue of the Drosophila discs large tumor suppressor protein. *Proc Natl Acad Sci U S A* 1997; **94**: 11612–11616.
29. Imabayashi H, Mori T, Gojo S, *et al.* Redifferentiation of dedifferentiated chondrocytes and chondrogenesis of human bone marrow stromal cells via chondrosphere formation with expression profiling by large-scale cDNA analysis. *Exp Cell Res* 2003; **288**: 35–50.
30. Naviaux RK, Costanzi E, Haas M, Verma IM. The pCL vector system: rapid production of helper-free, high-titer, recombinant retroviruses. *J Virol* 1996; **70**: 5701–5705.
31. Halbert CL, DG Galloway DA. The E7 gene of human papillomavirus type 16 is sufficient for immortalization of human epithelial cells. *J Virol* 1991; **65**: 473–478.
32. Cosset F-LTY, Battini J-L, Weiss RA, Collins MKL. High-titer packaging cells producing recombinant retroviruses resistant to human serum. *J Virol* 1995; **69**: 7430–7436.
33. Yamashita T, Tonoki H, Nakata D, Yamano S, Segawa K, Moriuchi T. Adenovirus type 5 E1A immortalizes primary rat cells expressing wild-type p53. *Microbiol Immunol* 1999; **43**: 1037–1044.
34. Tomita S, Nakatani T, Fukuhara S, Morisaki T, Yutani C, Kitamura S. Bone marrow stromal cells contract synchronously with cardiomyocytes in a co-culture system. *Jpn J Thorac Cardiovasc Surg* 2002; **50**: 321–324.
35. Kohyama J, Abe H, Shimazaki T, *et al.* Brain from bone: efficient "meta-differentiation" of marrow stroma-derived mature osteoblasts to neurons with Noggin or a demethylating agent. *Differentiation* 2001; **68**: 235–244.
36. Pittenger MF, Mackay AM, Beck SC, *et al.* Multilineage potential of adult human mesenchymal stem cells. *Science* 1999; **284**: 143–147.
37. Jiang Y, Jahagirdar BN, Reinhardt RL, *et al.* Pluripotency of mesenchymal stem cells derived from adult marrow. *Nature* 2002; **418**: 41–49.
38. Romanov SR, Kozakiewicz BK, Holst CR, Stampfer MR, Haupt LM, Tlsty TD. Normal human mammary epithelial cells spontaneously escape senescence and acquire genomic changes. *Nature* 2001; **409**: 633–637.
39. Rheinwald JG, Hahn WC, Ramsey MR, *et al.* A two-stage, p16(INK4A)- and p53-dependent keratinocyte senescence mechanism that limits replicative potential independent of telomere status. *Mol Cell Biol* 2002; **22**: 5157–5172.

40. Bodnar AG, Ouellette M, Frolkis M, *et al.* Extension of life-span by introduction of telomerase into normal human cells. *Science* 1998; **279**: 349–352.
41. Taylor S, Jones PA. Multiple new phenotypes induced in 10T1/2 cells and 3T3 cells treated with 5-azacytidine. *Cell* 1979; **17**: 771–779.
42. Santi DV, Norment A, Garrett CE. Covalent bond formation between a DNA-cytosine methyl transferase and DNA containing 5-azacytidine. *Proc Natl Acad Sci U S A* 1984; **81**: 6993–6997.
43. Tomita S, Li RK, Weisel RD, *et al.* Autologous transplantation of bone marrow cells improves damaged heart function. *Circulation* 1999; **100**: II247–256.
44. Terada N, Hamazaki T, Oka M, *et al.* Bone marrow cells adopt the phenotype of other cells by spontaneous cell fusion. *Nature* 2002; **416**: 542–545.
45. Zhang YM, Hartzell C, Narlow M, Dudley SC Jr. Stem cell-derived cardiomyocytes demonstrate arrhythmic potential. *Circulation* 2002; **106**: 1294–1299.
46. Linask KK, Knudsen KA, Gui YH. N-Cadherin-catenin interaction: necessary component of cardiac cell compartmentalization during early vertebrate heart development. *Dev Biol* 1997; **185**: 148–164.
47. Harigaya K, Handa H. Generation of functional clonal cell lines from human bone marrow stroma. *Proc Natl Acad Sci U S A* 1985; **82**: 3477–3480.

JOURNAL OF VIROLOGY, Jan. 2004, p. 104–115
0022-538X/04/$08.00+0 DOI: 10.1128/JVI.78.1.104–115.2004

Vol. 78, No. 1

Inhibition of S-Phase Cyclin-Dependent Kinase Activity Blocks Expression of Epstein-Barr Virus Immediate-Early and Early Genes, Preventing Viral Lytic Replication

Ayumi Kudoh,[1,2] Tohru Daikoku,[1] Yutaka Sugaya,[1] Hiroki Isomura,[1] Masatoshi Fujita,[3] Tohru Kiyono,[3] Yukihiro Nishiyama,[2] and Tatsuya Tsurumi[1]*

Division of Virology, Aichi Cancer Center Research Institute, Chikusa-ku, Nagoya 464-8681,[1] Virology Division, National Cancer Center, Chuo-ku, Tokyo 104-0045,[3] and Department of Virology, Nagoya University Graduate School of Medicine, Nagoya 466-8550,[2] Japan

Received 7 July 2003/Accepted 24 September 2003

The induction of lytic replication of the Epstein-Barr virus (EBV) completely arrests cell cycle progression, in spite of elevation of S-phase cyclin-dependent kinase (CDK) activity, thereby causing accumulation of hyperphosphorylated forms of retinoblastoma (Rb) protein (A. Kudoh, M. Fujita, T. Kiyono, K. Kuzushima, Y. Sugaya, S. Izuta, Y. Nishiyama, and T. Tsurumi, J. Virol. 77:851-861, 2003). Thus, the EBV lytic program appears to promote specific cell cycle-associated activity involved in the progression from G_1 to S phase. We have proposed that this provides a cellular environment that is advantageous for EBV productive infection. Purvalanol A and roscovitine, inhibitors of S-phase CDKs, blocked the viral lytic replication when cells were treated at the early stage of lytic infection, while well-characterized inhibitors of enzymes, such as mitogen-activated protein kinase, phosphatidylinositol 3-kinase, and protein kinase C, known to be involved in BZLF1 gene expression did not. Inhibition of CDK activity resulted in the accumulation of the hypophosphorylated form of Rb protein and inhibition of expression of EBV immediate-early and early proteins. Cycloheximide block-and-release experiments clearly demonstrated that even in the presence of enough amounts of the BZLF1 protein, purvalanol A blocked expression of lytic viral proteins at transcription level. Furthermore, reporter gene experiments confirmed that BZLF1-induced activation of early EBV promoters was impaired in the presence of the CDK inhibitor. We conclude here that the EBV lytic program promotes specific cell cycle-associated activity involved in the progression from G_1 to S phase because the S-phase-like cellular environment is essential for the expression of immediate-early and early genes supplying the viral replication proteins and hence for lytic viral replication.

The Epstein-Barr virus (EBV) is a B-lymphotropic gammaherpesvirus which is a causative agent of infectious mononucleosis known to be closely associated with several human cancers, including Burkitt's lymphoma and nasopharyngeal carcinoma, as well as lymphoproliferative disorders (16). Although infection by EBV occurs in most individuals, it is usually asymptomatic. The life cycle is quite distinct from those of other herpesviruses, such as herpes simplex virus type 1 (HSV-1) or cytomegalovirus (CMV), for which full lytic replication can be accomplished by infection of certain cell types. Such an efficient lytic replication system, however, does not exist for EBV. The virus specifically infects resting B lymphocytes, inducing the continuous proliferation of B cells (16), and the resulting lymphoblastoid cell lines (LCLs) express a limited number of EBV gene products, including six nuclear proteins (EBNA-1, EBNA-2, EBNA-3A, EBNA-3B, EBNA-3C, and EBNA-LP), three membrane proteins (LMP-1, LMP-2A, and LMP-2B), EBV-encoded small RNAs (EBER1 and EBER2), and transcripts from the *Bam*HI A region. They activate quiescent B cells to enter the cell cycle, maintain continuous proliferation, and prevent cells from undergoing apoptosis. The viral genome is maintained as covalently closed circular plasmids forming nucleosomal structures with histone proteins in the nuclei of the LCLs. The number of copies is maintained at 10 to 50 per cell, to be duplicated once during each cell division cycle by the host cellular DNA replication machinery (66).

Lytic replication differs from the latent amplification state in that multiple rounds of replication are initiated within oriLyt (23), and the replication process has a greater dependence on EBV-encoded replication proteins (18). EBV encodes seven viral replication genes. The BZLF1 protein acts as an oriLyt-binding protein as well as the immediate-early transactivator (50). The BALF5 gene encodes the DNA polymerase (Pol) catalytic subunit (59), and the BMRF1 gene encodes the DNA Pol accessory subunit (55–57). A single-stranded DNA-binding protein is encoded by the BALF2 gene (58, 61). The remaining three proteins encoded by the BBLF4, BSLF1, and BBLF2/3 genes form a tight complex (19, 67) and are predicted to act as helicase, primase, and helicase-primase-associated proteins, respectively, based on sequence homology to the HSV-1 UL5, UL52, and UL8 genes (18). These viral replication proteins, other than the BZLF1 protein, conceivably work together at replication forks to synthesize leading and lagging strands of the concatemeric EBV genome. Upon reactivation, the two key EBV immediate-early lytic genes, BZLF1 and BRLF1, are expressed. These genes encode transactivators that activate

* Corresponding author. Mailing address: Division of Virology, Aichi Cancer Center Research Institute, 1-1, Kanokoden, Chikusa-ku, Nagoya 464-8681, Japan. Phone: 81-52-764-2979. Fax: 81-52-764-2979. E-mail: ttsurumi@aichi-cc.jp.

viral and certain cellular promoters and lead to an ordered cascade of viral gene expression: activation of early gene expression followed by the lytic cascade of viral genome replication and late gene expression (16). In the viral productive cycle, the EBV genome is amplified more than 100-fold. Intermediates of viral DNA replication are found as large head-to-tail concatemeric molecules, probably resulting from rolling-circle DNA replication (23), which are subsequently cleaved into unit length genomes and packaged into virions in the nucleus.

The BZLF1 protein mediates the switch between the latent and lytic forms of EBV infection and alone is sufficient to activate the EBV lytic cascade (23). It has been demonstrated that it inhibits host cell proliferation by causing cell cycle arrest in G_0/G_1 in several epithelial tumor cell lines lacking the EBV genome (7, 43). Such G_0/G_1 arrest was found to result from induction of the tumor suppressor protein p53 and the cyclin-dependent kinase (CDK) inhibitors $p21^{WAF-1/CIP-1}$ and $p27^{KIP-1}$, followed by accumulation of the hypophosphorylated form of retinoblastoma (Rb) protein (7). Recently, it has been reported that the BZLF1 protein by itself activates E2F-1, cyclin E, and Cdc25A, which are involved in cell cycle progression in telomerase-immortalized human keratinocytes and primary tonsil keratinocytes but not in human fibroblasts (35). Furthermore, the other immediate-early transactivator BRLF1 protein can induce contact-inhibited, quiescent human fibroblasts to enter the S phase with dramatic increase in the level of E2F-1 (53). E2F-1 activates the transcription of many proteins involved in cellular DNA synthesis and cell cycle progression (1) and probably the transcription of the EBV DNA Pol gene as well (33). The available data suggest that E2F activity is required for lytic viral DNA replication.

In a previous study seeking to characterize cellular circumstances suitable for lytic replication in LCLs, we established a tetracycline-inducible expression system for the BZLF1 protein in the B95-8 B-lymphoblastoid cell line, which is latently infected with EBV and possesses normal p53 pathway (15, 30). The system is simple and highly efficient for conditional induction of the lytic replication program in the absence of any other external stimuli. As a result, it could be clearly demonstrated that induction of the BZLF1 protein results in arrest of cell cycle progression and inhibition of replication of cellular DNA simultaneous with induction of that for lytic viral DNA. Unexpectedly, although Tet-BZLF1/B95-8 cells harbor functional and responsive p53 and retain the ability to activate checkpoint pathways (30), the levels of p53 and the CDK inhibitors $p21^{WAF-1/CIP-1}$, $p27^{KIP-1}$, and $p16^{INK4a}$ were found to be constant before and after induction of the lytic program, in contrast to the results reported by Cayrol and Flemington (7). Rather, activation of S-phase-promoting CDK, i.e., cyclin E/A-CDK2, and accumulation of the hyperphosphorylated form of Rb protein were observed. Therefore, we speculated that the late G_1 or early S-arrested state induced by productive EBV infection provides a cellular environment that is advantageous for EBV replication in that metabolic precursors (i.e., nucleotides) are abundantly available for viral replication. Since cellular DNA synthesis is inhibited, there is no competition for viral access to these precursors.

Cellular CDKs comprise a family of serine-threonine protein kinases whose activity is regulated by association with specific cyclin partners, phosphorylation, and interaction with CDK inhibitors such as $p21^{waf1/cip1}$, $p27^{kip1}$, $p16^{ink4a}$, and $p15^{ink4b}$, whose expression is itself tightly controlled. With regard to the involvement of CDKs in DNA synthesis, activation of CDK-2 is necessary for expression of many cellular DNA replication proteins and CDK-2 phosphorylates and activates several of the cellular proteins that are required for DNA synthesis. Among the CDK2 targets, the Rb protein is most important for cell cycle progression. The present paradigm for phosphorylation regulation of Rb protein is as follows (6, 24, 27, 29). During early G_1, Rb is phosphorylated by cyclin D-CDK4/6, leading to cyclin E expression. Near the end of G_1, it becomes maximally hyperphosphorylated by cyclin E/CDK2, allowing cells to enter into S phase, and the hyperphosphorylated state is maintained by cyclins A/E-CDK2. In a previous study, Kudoh et al. found that hyperphosphorylated Rb proteins accumulate as lytic EBV infection proceeds (30). In particular, CDK2 phosphorylation of Ser612 in Rb continued to increase. Based on these observations, we speculated that cell cycle-related factors normally active in uninduced cells in the late G_1 or early S phase may be required for lytic replication of EBV. If this is indeed the case, inhibition of their activity should block viral replication. To test this hypothesis, we measured the effects on viral replication of two recently described CDK inhibitors, purvalanol A and roscovitine (22, 36). Both drugs inhibit CDK2 and CDK1 but not CDK4 or CDK6 or a large number of other kinases. They compete with ATP for binding to the ATP-binding pocket of the target CDKs, and all known effects of purvalanol A and roscovitine on cells can be attributed to the resultant inhibition of kinase activity of CDK2 and CDK1 (17, 21, 36, 51).

In the present study, we found that both purvalanol A and roscovitine block EBV lytic replication while well-characterized inhibitors of other protein kinases, such as mitogen-activated protein (MAP) kinase, phosphatidylinositol (PI) 3-kinase, and protein kinase C, do not. The effects of purvalanol A can be shown to be due to inhibition of expression of viral immediate-early and early proteins, including the replication proteins encoded by the BALF2, BALF5, BMRF1, and BBLF2/3 genes. We conclude that the EBV lytic program promotes specific cell cycle-associated activity involved in the progression from G_1 to S phase, because S-phase CDK activity appears to be essential for the expression of viral immediate-early and early lytic proteins and hence for lytic viral replication.

MATERIALS AND METHODS

Materials. Purvalanol A was purchased from Calbiochem (San Diego, Calif.) and roscovitine was obtained from Promega (Madison, Wis.), with stock solutions being prepared at concentrations of 10 mM in dimethyl sulfoxide (DMSO). Both are selective inhibitors of CDKs and have the following characteristics: purvalanol A, 2-(1-R-isopropyl-2-hydroxyethylamino)-6-(3-chloroanilino)-9-isopropylpurine, molecular weight of 388.9, 50% inhibitory concentrations (IC_{50}s) of 4 nM for CDK1/cyclin B, 70 nM for CDK2/cyclin A, 35 nM for CDK2/cyclin E, and 75 nM for CDK5/p35 (22); roscovitine, 2-(1-D,L-hydroxymethylpropylamino)-6-benzylamino-9-isopropylpurine, molecular weight of 354.4, IC_{50}s of 65 nM for CDK1/cyclin B, 700 nM for CDK2/cyclin A, 700 nM for CDK2/cyclin E, and 200 nM for CDK5/p35. Roscovitine exhibits reduced sensitivity towards related kinases, including ERK1 and ERK2 (IC_{50}s of 30 and 14 μM, respectively) and does not significantly affect the activities of other protein kinases, including CDK4/cyclin D and CDK6/cyclin E, even at a concentration of 100 μM (3, 36). LY-294002, mevinolin, bisindolylmaleimide I, and cycloheximide were purchased from Sigma. LY-294002 [2-(4-morpholinyl)-8-phenyl-4H-1-benzopyran-4-one], a

specific PI 3-kinase inhibitor, was dissolved in DMSO at a concentration of 20 mM. Mevinolin, a drug that specifically inhibits MAP kinase (ERK1 and ERK2) but not CDKs, was diluted in ethanol to a concentration of 20 mM. Bisindolylmaleimide I (2-[1-(3-dimethylaminopropyl)-1H-indol-3-yl]-3-(1H-indol-3-yl)-maleimide) (molecular weight, 412.5), a broad-spectrum protein kinase C inhibitor that is structurally similar to staurosporine, was stored in DMSO at a concentration of 10 mM. It shows high selectivity for protein kinase C (K_i = 10 nM) and may inhibit protein kinase A at a much higher concentration (K_i = 2 μM) (54). Cycloheximide, a specific inhibitor of protein synthesis which works by preventing translocation of ribosomes, was diluted in ethanol to a concentration of 50 mg/ml.

Stocks of all drugs were aliquoted and kept at −20°C until use. The final concentration of each drug used is indicated in the figure legends.

Cells. Kudoh et al. previously reported that the exogenous BZLF1 protein is conditionally expressed under the control of a tetracycline-regulated promoter in Tet-BZLF1/B95-8 cells, a marmoset B-cell line latently infected with EBV (30). Tet-BZLF1/B95-8 cells and Tet-BZLF1/Akata cells were maintained in RPMI medium supplemented with 1 μg of puromycin/ml, 250 μg of hygromycin B/ml, and 10% tetracycline-free fetal calf serum at 37°C in a humidified atmosphere containing 5% CO_2. To induce lytic EBV replication, the tetracycline derivative doxycycline was added to the culture medium at a final concentration of 1 to 5 μg/ml.

Establishment of Tet-BZLF1/Akata cells. Akata cells, human EBV-positive Burkitt's lymphoma cells, were infected with the stocks of recombinant retrovirus, rv-BZLF1 and rv-rtTA, as described previously (30). Clones resistant to puromycin and hygromycin B were isolated by limiting dilution and checked for expression of the BZLF1 and BALF2 proteins with doxycycline by Western blot analysis.

Establishment of Tet-BZLF1/HeLa. The plasmid pCMSCV-RevTRE(hyg)-BZLF1 (30) was transfected into HeLa Tet-on cells expressing rtTA (Clontech). One day later, cells were plated in selective medium containing 250 μg of hygromycin B/ml and 100 μg of G418/ml. Several clones expressing BZLF1 protein with doxycycline were isolated, and one was used for the present study. The Tet-BZLF1 HeLa cell was cultured in Dulbecco's modified Eagle's medium containing 10% tetracycline-free fetal calf serum, hygromycin B (250 μg/ml), and G418 (100 μg/ml). To induce BZLF1 protein expression, doxycycline was added to the culture medium at a final concentration of 5 μg/ml.

Transfections and CAT assays. Approximately 5×10^5 Tet-BZLF1/HeLa cells were plated in 60-mm-diameter dishes. Cells were transfected with 2 μg of pBMRF1-CAT or pBHRF1-CAT (8, 68) by using Lipofectamine with Plus reagent (Invitrogen) according to the manufacturer's instructions. Media were replaced at 16 h posttransfection with fresh media containing or free of purvalanol A (20 μM). Twenty hours posttransfection, doxycycline was added to a final concentration of 5 μg/ml or not. Forty-eight hours after addition of doxycycline, cells were harvested and treated with Reporter lysis buffer (Promega) for 15 min. After incubation, the samples were heated at 60°C for 10 min to inactivate endogenous deacetylase activity. Chloramphenicol acetyltransferase (CAT) activity was assayed by incubating each sample with *n*-butyryl coenzyme A and [^{14}C]chloramphenicol at 37°C for 3 h according to the manufacturer's instructions (Promega). The reaction product, *n*-butyryl [^{14}C]chloramphenicol, was selectively extracted with 300 μl of xylene. The xylene phase was mixed with scintillation cocktail, and the radioactivity of the product was measured with a scintillation counter.

Quantification of viral DNA synthesis during lytic replication. Tet-BZLF1/B95-8 cells were incubated with or without 1 μg of doxycycline/ml in the presence or absence of the indicated drugs and harvested at the indicated times. Total DNAs from a total of 3.5×10^6 Tet-BZLF1/B95-8 cells were purified with a DNeasy Tissue kit (Qiagen) and quantified. Diluted amounts of DNA samples were dot-blotted on a Hybond-N membrane (Amersham) and hybridized with a ^{32}P-labeled DNA fragment consisting of a portion of the EBV EBNA1 coding region (EBV nucleotides 109110 to 109379). Signal intensity was quantified with an Image guider (BAS2500; Fujifilm). A standard curve for viral DNA quantification was obtained from serial dilutions of a plasmid, p500, which harbors an EBNA1 coding region. The copy numbers of viral genome per cell were determined from the standard curve and serial dilutions of DNA from Raji cells in which about 45 copies of viral genome per cell are present (11). DNA from BJAB cells was also used as a negative control.

Quantification of viral and host RNA transcripts during lytic replication. Tet-BZLF1/B95-8 cells were incubated with 5 μg of doxycycline/ml in the presence or absence of the indicated drugs and harvested at the indicated times. Total RNA was isolated from a total of 10^7 cells with an RNeasy mini kit (Qiagen). The RNA concentration was measured spectrophotometrically, assuming that 1 A_{260} is equal to a concentration of 40 μg/ml. Samples were stored at −80°C without detectable signs of degradation. RNA samples (5 μg) were size-fractionated on a 1.2% formaldehyde-agarose gel in morpholinepropanesulfonic acid (MOPS) running buffer and transferred to a Hybond-N+ membrane (Amersham). The membrane filters were hybridized at 65°C with ^{32}P-labeled probes obtained by PCR amplification of each viral and cellular DNA with the following primers: BZLF1, 5′-cacgggaccgatccagcct-3′ and 3′-atcgatgtt aacaagcttg-5′; BRLF1, 5′-gttccagactatggtctcgt-3′ and 3′-tatccaaggctgttcaggtt-5′; BALF5, 5′-ccccaactccagatgctcaagggt-3′ and 3′-agcagatccatgaccagg-5′; BMRF1, 5′-cgggatccatggaaaccactcagactctc-3′ and 3′-gtggtacaahagcgttcgcttaagg-5′; 36B4, 5′-ctggagaaactgctgcctcatatccg-3′ and 3′-ccaaatcccatatcctcgtccga-5′. Signal intensity was quantified with an Image guider (BAS2500; Fujifilm). The levels of the specific viral and cellular gene transcripts were plotted and compared with those prior to treatment with the drugs.

Protein preparation. Tet-BZLF1/B95-8 cells were harvested at the indicated times postinduction with or without doxycycline, washed with phosphate-buffered saline (PBS), and treated with lysis buffer (0.02% sodium dodecyl sulfate [SDS], 0.5% Triton X-100, 300 mM NaCl, 20 mM Tris-HCl [pH 7.6], 1 mM EDTA, 1 mM dithiothreitol, 10 μg of leupeptin/ml, 5 μg of pepstatin A/ml) for 20 min on ice. Samples were centrifuged at 18,000 × *g* for 10 min at 4°C, and the clarified cell extracts were measured for protein concentrations by using a Bio-Rad protein assay kit.

Immunoblot analysis. Twenty micrograms of proteins was loaded in each lane for SDS–10% polyacrylamide (acrylamide/bisacrylamide ratio = 29.2:0.8) gel electrophoresis (PAGE). To separate phosphorylated forms of Rb proteins, proteins were subjected to SDS–7.5% PAGE (acrylamide/bisacrylamide ratio = 60:1) and then transferred to polyvinylidene difluoride membranes. The membranes were washed with blotting buffer (1× PBS containing 0.1% Tween 20), blocked for 60 min in blotting buffer containing 10% low-fat powdered milk, washed once with blotting buffer, and incubated at room temperature for 60 min with primary antibodies in blotting buffer containing 5% low-fat powdered milk. They were then further washed in blotting buffer and incubated with horseradish peroxidase-conjugated secondary antibody at room temperature for 60 min. The target proteins were detected with an enhanced chemiluminescence detection system (Amersham). Images were processed by LumiVision PRO (Aisin/Taitec, Inc.) with a cooled charge-coupled device (CCD) camera and assembled using an Apple G4 computer with Adobe Photoshop 5.0. Signal intensities were quantified with a LumiVision image analyzer. The system used in this study features a cooled CCD camera that has a 16 bit = 65,535 grayscale wide dynamic range. The accuracy of the quantitative analysis was enhanced up to 100 times compared with the standard quantitative analysis scanning X-ray film.

Antibodies. Preparation and specificities of the anti-BZLF1 protein-specific, anti-BALF2 protein-specific, anti-BALF5 protein-specific, and anti-BBLF2/3 protein-specific polyclonal antibodies were described previously (59, 60, 67). An anti-BMRF1 protein-specific monoclonal antibody, clone name R3, was purchased from Chemicon, and an anti-BRLF1-specific antibody was obtained from Argen, Inc. The anti-Rb-specific monoclonal antibody was purchased from Becton Dickonson Transduction Laboratories and the anti-phospho-Rb (Ser612)-specific monoclonal antibody was the kind gift of Katsuyuki Tamai (MBL, Inc.). Anti-PCNA antibody was commercially obtained from MBL, Inc.

RESULTS

In a recent study, Kudoh et al. isolated Tet-BZLF1/B95-8 cells in which the exogenous BZLF1 protein was conditionally expressed under the control of a tetracycline-regulated promoter (30). More than 80% of Tet-BZLF1/B95-8 cells became positive for BZLF1 and BMRF1 proteins 48 h after doxycycline annexation. The copy number of the viral genome in the cells was significantly amplified after 24 h postinduction. Thus, the system is simple and highly efficient for conditional induction of the lytic replication program in the absence of any other external stimuli, allowing use for further analyses.

S-phase CDK inhibitors purvalanol A and roscovitine completely inhibit lytic EBV replication. The previous study by Kudoh et al. indicated that the EBV lytic program promotes post-restriction point characteristics, including high CDK2 activity and hyperphosphorylation of the Rb protein (30). This finding suggests the possibility that S-phase CDK activity or free E2F released from the Rb-E2F complex due to hyper-

phosphorylation of the Rb protein is required for lytic EBV replication. If this were the case, then inhibition of CDK2 activity, which would thereby prevent phosphorylation of Rb protein, would result in inhibition of EBV productive infection. Roscovitine (36) and purvalanol A (22) are the 2,6,9-trisubstituted purine-derived pharmacological CDK inhibitors which have been best characterized so far. Both drugs inhibit CDKs 1 and 2 with high potency, but they do not inhibit CDKs 4 or 6 or a number of other kinases.

To clarify the effects of purvalanol A and roscovitine on the progression of EBV lytic replication, Tet-BZLF1/B95-8 cells were treated with doxycycline in the presence or absence of either drug. Total DNA was extracted from the cells, and the EBV DNA-specific signal was quantitated. The copy number of the EBV genome per Tet-BZLF1/B95-8 cell was calculated to be about 40 before treatment with doxycycline. In the absence of kinase inhibitors, the copy number of the viral DNA was amplified to more than 9,000 per cell after 72 h postinduction. As shown in Fig. 1A, 15 μM purvalanol A and 50 μM roscovitine blocked lytic replication of EBV almost completely throughout the 72-h period. No obvious cytotoxic effects were observed by microscopic evaluation when uninduced Tet-BZLF1/B95-8 cells were treated with concentrations of purvalanol A up to 50 μM (data not shown).

The specificities of purvalanol A and roscovitine have been evaluated so extensively that these drugs are presently used to confirm the involvement of CDKs in biological processes (4, 17, 21, 36, 46, 47, 49, 51). However, it remained a theoretical possibility that our findings with purvalanol A and roscovitine were the consequence of a block of another cellular protein serine/threonine kinase(s) such as protein kinase C, PI 3-kinase, or MAP kinase. These are known to be activated on the occasion of a switch from latent to lytic infection of EBV, leading to expression of the BZLF1 protein in vivo (9, 20). Indeed, roscovitine also inhibits MAP kinase (ERK1 and -2) (although ~20- and ~10-fold less efficiently, respectively, than for CDKs). We also investigated whether these kinases are required for lytic EBV replication in the Tet-on expression system. As shown in Fig. 1A, mevinolin, a drug that specifically inhibits ERK1 and -2 but not CDKs (14), did not inhibit EBV lytic replication at a concentration of 20 μM. Similarly, the PI 3-kinase inhibitor LY-294002 did not block the lytic replication at all at a concentration of 15 μM. Further, there appeared to be a moderate inhibition of EBV lytic infection with bisindolylmaleimide I, a broad-spectrum protein kinase C inhibitor, at a concentration of 10 μM. Since protein kinase C increases early in lytic cycle promoter activity (32), the addition of protein kinase C inhibitor to the culture appears to hinder the productive replication moderately. As shown in Fig. 1B, purvalanol A, mevinolin, LY-294002, and bisindolylmaleimide I did prevent cell proliferation completely at the concentrations utilized.

Thus, lytic EBV replication was inhibited only by inhibitors of S-phase CDKs and not by those of PI 3-kinase, MAP kinase, and protein kinase C.

Inhibition of lytic EBV replication by purvalanol A is not mediated by irreversible drug-induced cytotoxicity. Although purvalanol A and roscovitine did not induce detectable cytopathology, as determined by microscopic evaluation, at the concentrations used to block EBV replication (data not shown), it remained a possibility that more subtle but irrevers-

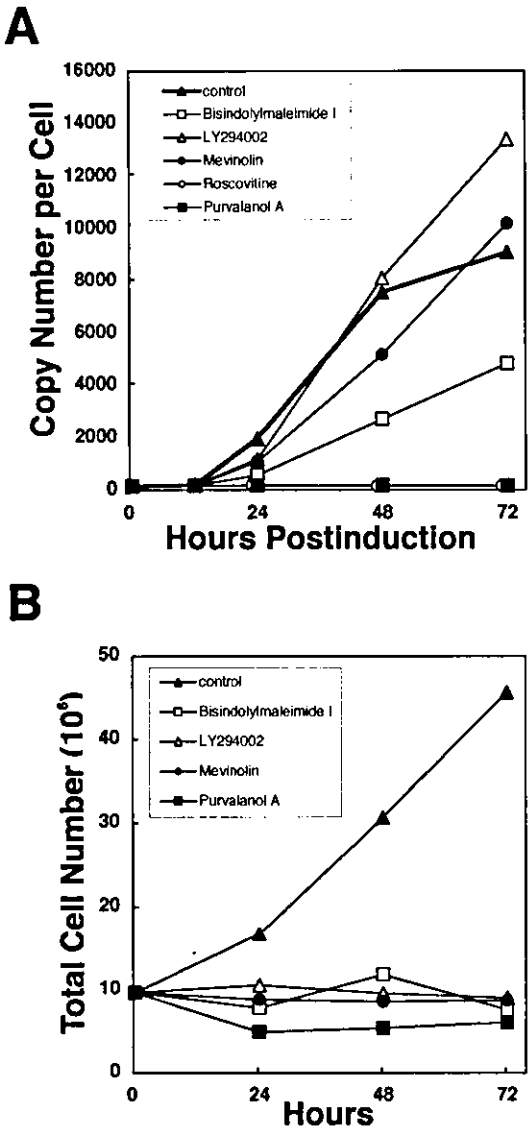

FIG. 1. (A) Specific inhibition of EBV lytic replication by the CDK inhibitors roscovitine and purvalanol A. Tet-BZLF1/B95-8 cells were cultured in the presence of 1 μg of doxycycline/ml with drug-free medium (control) or media containing each indicated drug and harvested at the indicated times. The drug concentrations used in the experiments were as follows: 10 μM bisindolylmaleimide I, 15 μM LY-294002, 20 μM mevinolin, 50 μM roscovitine, and 15 μM purvalanol A. To determine viral DNA synthesis, slot blot assays for viral DNA were performed as described in Materials and Methods. Signal intensity was quantified with an Image guider (Fujifilm), and the copy numbers of viral genome per cell were calculated. (B) Effect of bisindolylmaleimide I, LY-294002, mevinolin, and purvalanol A on the proliferation of Tet-BZLF1/B95-8 cells. Tet-BZLF1/B95-8 cells were seeded in flasks (10^7 cells/flask) with drug-free medium (control) or media containing each indicated drug. The numbers of cells were counted with a hemocytometer at the indicated times, and the data were plotted in the graph. The drug concentrations used in the experiments were the same as those described for panel A.

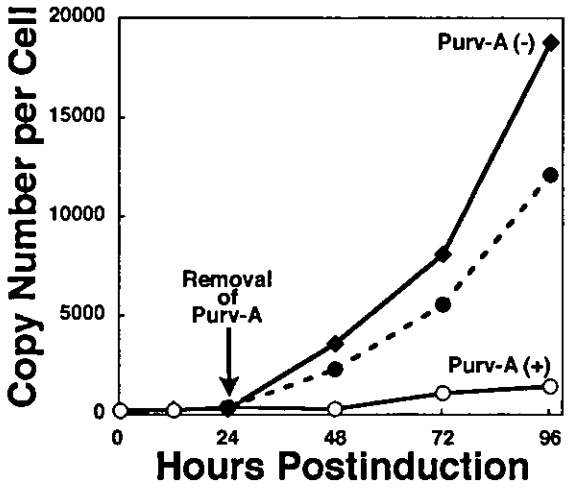

FIG. 2. Inhibition of EBV lytic replication by purvalanol A is reversible. Tet-BZLF1/B95-8 cells were cultured with doxycycline (1 μg/ml) in the presence (○, ●) or absence (◆) of purvalanol A (15 μM). Aliquots of cells treated with purvalanol A were also transferred to purvalanol A-free fresh medium at 24 h postinduction (dashed line). This medium change is indicated by the arrow. Cells were harvested at the indicated times, and viral DNA synthesis was determined by slot blot assay as described in Materials and Methods.

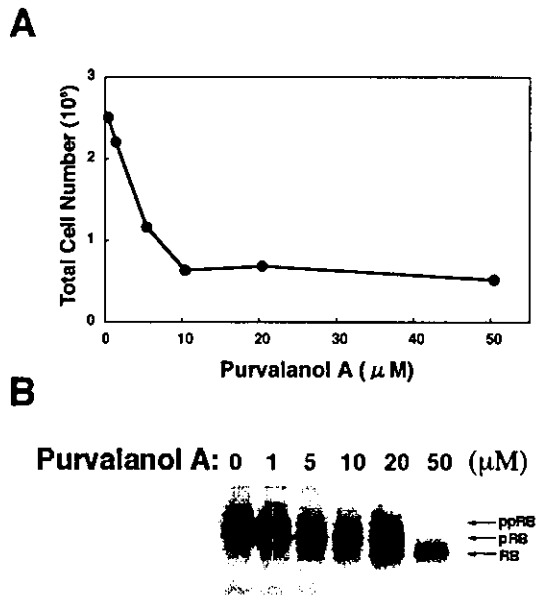

FIG. 3. (A) Dose dependence of purvalanol A effects on the proliferation of Tet-BZLF1/B95-8 cells. Tet-BZLF1/B95-8 cells were seeded in 35-mm-diameter petri dishes (1.0×10^6 cells/dish). The cells were incubated for 48 h in RPMI 1640 medium containing the indicated concentrations of purvalanol A. The cells were harvested, and total cell numbers were counted with a hemocytometer. (B) Effects of purvalanol A on the phosphorylation state of Rb protein. Cells were cultured in the presence of indicated concentrations of purvalanol A and harvested after 48 h. Clarified cell lysates were prepared, separated by SDS–7.5% PAGE, and applied for Western blot analyses with anti-Rb protein polyclonal antibody. pRB and ppRB are slower-migrating hyperphosphorylated forms of Rb protein. The faster-migrating band is the hypophosphorylated form of Rb protein and is designated as RB.

ible toxic effects of these drugs may have compromised the ability of cells to support lytic EBV replication. To determine whether this was the case, we performed a purvalanol A reversal experiment. Purvalanol A was selected for these experiments because it inhibits EBV replication efficiently at a lower concentration than does roscovitine. Tet-BZLF1/B95-8 cells treated with doxycycline were cultured in the presence of 15 μM purvalanol A for 24 h, and the medium was replaced with purvalanol A-free fresh medium. At the indicated times, cells were harvested and the copy numbers of viral genome DNA were calculated by a standard Southern blot hybridization assay (Fig. 2). When the medium was replaced with fresh medium containing purvalanol A, the copy number of the viral genome per cell did not increase. In contrast, after release from the purvalanol A block, resumption of EBV lytic replication was evident in the cells (Fig. 2).

We conclude from these experiments that purvalanol A-induced inhibition of EBV lytic replication is not mediated by irreversible drug-induced toxicity in Tet-BZLF1/B95-8 cells.

Purvalanol A prevents cell proliferation in inverse proportion to the phosphorylation state of Rb protein. As shown in Fig. 3A, proliferation of Tet-BZLF1/B95-8 cells was inhibited by the CDK inhibitor purvalanol A at concentrations greater than 5 μM. Since the compound inhibits CDK2 and CDK1 activity selectively, the phosphorylation states of Rb protein in Tet-BZLF1/B95-8 cells were drastically changed as the concentration of purvalanol A was increased in the medium (Fig. 3B), i.e., the hypophosphorylated form of Rb protein was increased in a dose-dependent manner (Fig. 3B). Cell growth inhibition by purvalanol A appeared to be in proportion to the ratio of the hypophosphorylated to hyperphosphorylated forms of the Rb protein (compare Fig. 3A and B). More than 90 percent of the Tet-BZLF1/B95-8 cells treated with purvalanol A were in G_1 phase by fluorescence-activated cell sorter analysis (data not shown). Collectively, these observations indicate that the cellular condition of G_1 phase induced by purvalanol A is not favorable for induction of lytic replication of EBV.

Purvalanol A and roscovitine inhibit EBV lytic replication when added until 9 h postinduction. To determine whether CDKs are required for essential EBV functions that occur after expression of the BZLF1 protein, we evaluated the effects on viral replication of adding purvalanol A at selected times after annexation of doxycycline. Two recognized cellular targets of purvalanol A are CDK-1 and CDK-2. Since CDK-2 is involved in cellular DNA replication (12), we determined whether CDK-2 might also participate in viral DNA replication directly. If this were the case, then purvalanol A or roscovitine would inhibit the lytic phase of viral DNA replication even in the presence of viral replication proteins. To test this hypothesis, after addition of doxycycline to the culture medium, either purvalanol A or roscovitine was added at the indicated times. Cells were harvested at 72 h posttreatment with doxycycline, and the copy number of EBV genomes was calculated (Fig. 4). No CDK inhibitor was added to control cultures. As shown in Fig. 4, the addition of purvalanol A or roscovitine immediately after doxycycline treatment resulted in an almost total block in EBV lytic replication throughout the

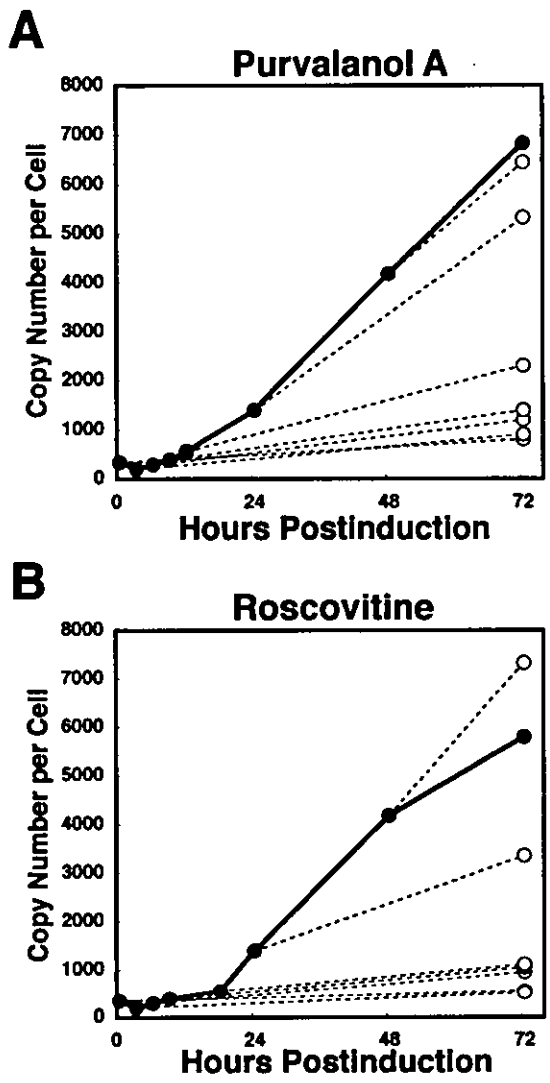

FIG. 4. The CDK inhibitors purvalanol A and roscovitine inhibit EBV lytic replication when added at least until 9 h postinduction. Tet-BZLF1/B95-8 cells were treated with 1 μg of doxycycline/ml for 72 h. Purvalanol A (15 μM) (A) or roscovitine (50 μM) (B) was added at the indicated times (0, 3, 6, 9, 24, and 48 h) postinduction, and the cells were harvested at 72 h postinduction and viral DNA synthesis was determined by slot blot assay as described in Materials and Methods (dashed lines, O). Signal intensity was quantified with an Image guider (Fujifilm). An additional series of Tet-BZLF1/B95-8 cells with productive infection was incubated continuously in CDK inhibitor-free medium and harvested at the indicated times (control; ●).

72-h period. The addition of purvalanol A or roscovitine at 3, 6, and 9 h postinduction had nearly identical inhibitory effects on viral replication (Fig. 4). However, viral genome synthesis by lytic EBV replication was not markedly inhibited when purvalanol A was added to the culture medium 24 h postannexation, although there was a moderate inhibition of viral genome synthesis at 24 h postinduction with roscovitine (Fig. 4). Until 24 h postinduction, viral replication proteins were expressed at near plateau levels sufficient for synthesis of the viral genome in Tet-BZLF1/B95-8 cells (Fig. 5B, lanes 5 and 6). These results strongly suggest that cellular CDKs sensitive to drugs are not directly involved in the lytic phase of viral DNA replication after viral replication proteins are already expressed but rather affect viral function(s) at early stages of the lytic replication.

Accumulation of viral immediate-early and early proteins is significantly reduced in the presence of purvalanol A. Since purvalanol A inhibits lytic EBV replication when added at least until 9 h after induction of the lytic program (Fig. 4A), we hypothesized that it may inhibit an (relatively) early stage of viral function. Lytic viral DNA synthesis requires previous immediate-early and early gene expression for supply of viral replication proteins and consequently occurs later in the infection cycle. To determine whether viral gene expression was impaired by purvalanol A, the following experiments were designed. Tet-BZLF1/B95-8 cells were treated with doxycycline in the presence or absence of purvalanol A, and total cell extracts were prepared at the indicated times postinduction. As shown in Fig. 5A, the phosphorylation states of Rb protein drastically changed in Tet-BZLF1/B95-8 cells treated with doxycycline as well as untreated cells (Fig. 3). In the absence of purvalanol A, almost all Rb protein became hyperphosphorylated at 48 h postinduction, as was observed previously (30). Ser612 of Rb protein is known to be preferentially phosphorylated by cyclin E/A-CDK2 (52). As shown in Fig. 5B, lane 6, phosphorylation of Ser612 in Rb protein was conspicuous. In contrast, with the addition of purvalanol A, Rb protein was hypophosphorylated within 4 h after treatment and this continued throughout 48 h postinduction in both the doxycycline-treated and untreated Tet-BZLF1/B95-8 cells (Fig. 5A, compare lane 1 with lanes 4 and 5 or lanes 6 and 7). Also, phosphorylation of Ser612 in Rb protein was clearly inhibited by purvalanol A treatment (Fig. 5B, compare lane 6 with lane 7). On the other hand, levels of PCNA (as a control) were constant in the presence or absence of purvalanol A (Fig. 5B).

As shown in Fig. 5B, lane 7, the BZLF1 protein was expressed in the presence of purvalanol A, although the level was somewhat reduced compared with that in the absence of the drug. It should be noted that, since the BZLF1 protein itself activates expression of its own gene (2), the total amount is a sum of the Tet-on and endogenously expressed protein. Thus, it appears that the former conditional expression is not markedly affected by purvalanol A.

Expression of the other immediate-early protein, BRLF1, and early viral proteins such as the BALF2, BALF5, BBLF2/3, and BMRF1 proteins was, however, greatly inhibited by purvalanol A treatment, whereas the cellular protein PCNA was largely unaffected (Fig. 5B, compare lane 6 with lane 7). As expected, cells in purvalanol A-free medium synthesized viral immediate-early as well as early proteins during the same period (Fig. 5B, lane 6). Also, when cells treated with doxycycline were overlaid with purvalanol A-containing medium at 3 h postannexation, viral protein synthesis was significantly prevented for 48 h (Fig. 5B, lane 8). When purvalanol A was added to the culture at 9 h postinduction, BRLF1, BALF2, BALF5, BBLF2/3, and BMRF1 proteins were expressed to some extent but at low levels. At 9 h posttreatment with doxycycline in the absence of purvalanol A, the levels of the BRLF1, BALF2, BALF5, BBLF2/3, and BMRF1 proteins were very low (Fig. 5B, lane 4). Since viral immediate-early and